ABERRANT PALEOMAGNETIC DIRECTIONS IN THE CANADIAN CORDILLERA

by

GUY MARQUIS

B.Sc., Université du Québec à Chicoutimi, 1986

A THESIS SUBMITTED IN PARTIAL FULFILLEMENT

OF THE REQUIREMENTS FOR THE DEGREE OF

MASTER OF SCIENCE

in the department

of

Physics

ACCEPTED
FACULTY OF GRADUATE STUDIES
[redacted]
DEAN
DATE 02 June 1988

We accept this thesis as conforming
to the required standard

[redacted]
(E. Irving)

[redacted]
(John T. Weaver)

[redacted]
(Eileen Van der Flier-Keller)

[redacted]
(Nicholas D. Massey)

University of Victoria

Supervisor: Professor E. Irving

ABSTRACT

Paleomagnetism has been applied to two general tectonic problems in the Canadian Cordillera : post-Late Cretaceous latitudinal displacement of allochtonous terranes, and Eocene extension in the Omineca Belt. Aberrant paleomagnetic directions were observed in the Late Cretaceous Carmacks group (70.2 +/- 2.4 Ma), which comprises gently-dipping basaltic and andesitic lava flows overlying volcaniclastics deposits in southern Yukon and northwestern British Columbia. Volcanic sections which overlie Stikinia and Cache Creek terranes were sampled in three regions spread over 300 km. This area lies west of the Tintina-Northern Rocky Mountain Trench fault and east of the Denali-Shakwak fault. The Carmacks group provides some of the first paleomagnetic data from pre-Tertiary volcanic units in the northern Canadian Cordillera. AF and thermal demagnetizations revealed stable components for 18 of the 27 sites collected. Both polarities are observed. The site-mean direction (D = 166.7°, I = -71.4°, α_{95} = 4.8°) is pre-folding and so the magnetization is probably primary (i.e. latest Cretaceous). This gives a paleopole at 106.9°E, 82.5°N, A_{95} = 7.9°, leading to a northward displacement of 13.4° +/- 8.5° (1500+/-950 km).

This is consistent with the shallow paleolatitudes observed for somewhat older units in the Coast Plutonic Complex and is well accommodated by displacement estimates along the Northern Rocky Mountain Trench and associated lineaments, and by terrane motion models in the north Pacific Basin.

Aberrant paleomagnetic directions are also observed in Eocene intrusive rocks from the southern Omineca Belt, in southern British Columbia. Since these were fixed in their present positions, the aberrancies observed have to be caused by crustal tilting resulting from brittle normal faulting (domino effect). To the west of the Kettle-Grand Forks metamorphic complex, the Granby Pluton is tilted to the east by 38° +/- 9°. Within the complex, the Coryell Batholith is tilted to the east by 40° +/- 11°. To the east, high-grade metamorphic rocks 10 km west of Castlegar are tilted to the west by 39° +/- 5°. These results show that paleomagnetism can be used to determine tilt in plutonic rocks, which usually contain no signature of the paleohorizontal.

Examiners:

[redacted]

(E. Irving) (Eileen Van der Flier-Keller)

[redacted]

(John T. Weaver) (Nicholas D. Massey)

TABLE OF CONTENTS

LIST OF TABLES

LIST OF FIGURES

ACKNOWLEDGEMENTS

I first want to thank my supervisor, Dr E. IRVING, who introduced me to paleomagnetism, provided advice, support and encouragement throughout my two years in Victoria. He also spent the second field season with me, in south British Columbia. Thanks to Dr Brian R. GLOBERMAN, who brought me in the field for the first time in the Yukon and with whom I wrote my first paper (Chapter II of the thesis). To Jane WYNNE, who rushed me to Saltspring Island as I stepped out of the plane from Chicoutimi, and who also introduced me to the lab equipment. I benefited greatly from discussions with these three people and from their enthusiasm. I also want to thank Ms Sharon CARR, Dr J.T. FYLES and Dr Randall PARRISH for useful geological discussions. Funding from NSERC (grant to E. Irving) and from Fonds FCAR (scholarship) is also acknowledged.

DEDICATION

A mes parents, Gilles et Géraldine, qui m'ont laissé choisir mon avenir, et qui m'ont toujours encouragé dans tout ce que j'ai entrepris.

CHAPTER I GENERAL INTRODUCTION

Paleomagnetism is the study of the past geomagnetic field as recorded by the remanent magnetization of rocks. There are many ways a rock can acquire magnetization. Magnetization acquired by cooling the rock from high temperatures through the Curie points of the magnetic minerals is called thermoremanent magnetization (TRM). The Curie point is the highest temperature at which a material can retain magnetization. If the magnetization is acquired by chemical action during the formation of iron oxides at low temperatures, as they grow through their blocking diameter, it is called chemical remanent magnetization (CRM). If a non-geomagnetic field (i.e. those accompanying lightning strikes) remagnetized instantly the magnetic minerals at low temperatures, it is called isothermal remanent magnetization (IRM). If the magnetization is acquired while the rock stayed in a magnetic field for a long time at low temperatures, it is called viscous remanent magnetization (VRM).

Stability is controlled by the shape and the size of the grains of magnetic minerals and by their composition. An elongated grain magnetized along its axis will have stable remanent magnetization. A spherical grain will be less stable, i.e. its original magnetization will decay more rapidly. Because of the presence of internal self-demagnetizing fields, a large

magnetized grain will divide itself into smaller sections (magnetic domains with different orientations of magnetization) in order to minimize its total magnetic energy. This will make the magnetization in larger multi-domain grains much less stable than in smaller single-domain grains.

The results of a paleomagnetic study of many sites spaced through a thick rock sequence can be expressed by three numbers : D, the declination of the mean direction measured clockwise from north; I, its inclination below the horizontal; and α_{95}, the radius of a cone containing the mean paleomagnetic direction vector at a 95% confidence. If the magnetization is stable, then D, I is the mean direction of the geomagnetic field during the time the rocks were deposited. The intensity of magnetization is also determined, but this has a complex relation to the intensity of the geomagnetic field, which, in this thesis, has not been a subject of study.

The direction (D, I) can then be converted into a paleopole (Figs. 1 and 2). This calculation is based on the assumption that the geomagnetic field averaged over a sufficient period of time is, essentially, a geocentric axial dipole (GAD) field; that is, the mean geomagnetic pole coincides with the geographic pole. A time-average is needed to minimise the effects of the secular variation caused by non-dipole components of the field

MAPPING A PALEOMAGNETIC DIRECTION (I, D) AT A SITE

(θ_s, ϕ_s) TO A PALEOMAGNETIC POLE (θ_p, ϕ_p)

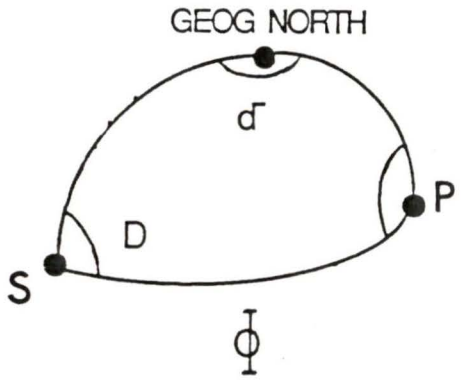

$$\theta_p = \sin^{-1} (\sin \theta_s \cos \Phi + \cos \theta_s \sin \Phi \cos D)$$

$$\phi_p = \phi_s + \delta$$

Where

$$\Phi = \cot^{-1} (\tan I/2)$$

$$\delta = \sin^{-1} (\cos \Phi \sin D/\cos \theta_p)$$

Figure 1. Mapping a direction to a paleomagnetic pole

MAPPING A PALEOMAGNETIC POLE (θ_p, ϕ_p) AT A SITE (θ_s, ϕ_s)

TO A PALEOMAGNETIC DIRECTION (D, I)

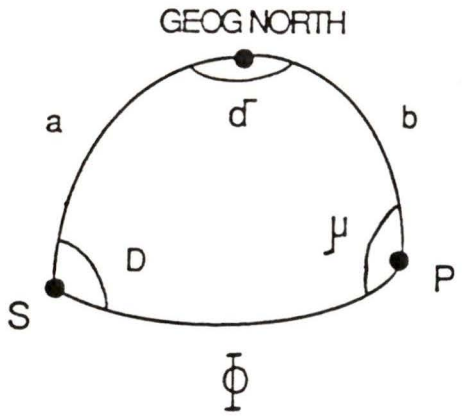

$a = 90^{o} - \theta_s$

$b = 90^{o} - \theta_p$

$\delta = \phi_p - \phi_s$

Using Napier's analogies

$$\tan (\mu - D)/2 = \frac{\cot(\delta/2) \sin (a-b)/2}{\sin (a+b)/2} = X$$

$$\tan (\mu + D)/2 = \frac{\cot(\delta/2) \cos (a-b)/2}{\cos (a+b)/2} = X'$$

$$D = \tan^{-1}X - \tan^{-1}X'$$

$$I = \tan^{-1} (2 \cot \Phi)$$

$$\Phi = \sin^{-1}(\sin \delta \ \sin b/\sin D)$$

Figure 2. Mapping a paleomagnetic pole to a direction

on a time-scale of 100 to 10 000 years. All the paleomagnetic poles for a given interval of time obtained for one plate can then be averaged to give the reference pole for that plate for that interval of time. A sequence of reference poles for successive time intervals makes an apparent polar wander (APW) path for that plate or craton.

Most poles observed from the Cordillera are offset from the APW path for the North American plate. The first discovery of an aberrant paleomagnetic field in the Cordillera was made by Cox (1957), in the early Eocene Siletz River volcanics in the Coast Range of western Oregon. Cox's interpretation was that the pole had wandered rapidly during Tertiary time, but Irving (1964) reinterpreted his data by rotating the Oregon Coast Range in such a way that the aberrant paleofield coincided with the reference field for North America; that is, the data indicated tectonic rotation not a rapid polar motion. Later, Beck (1976) reviewed the data and showed that most of the aberrant directions reported in the literature were from sampling sites in the Cordillera. He noted that generally the observed inclinations were shallower and/or the declinations were clockwise from the expected direction.

Such aberrant paleomagnetic directions can have

several causes, - they reflect one or more of three types of motion - tilting, translation or rotation (Figs. 3 to 5). Aberrant inclinations can be caused by latitudinal motions relative to the craton (Fig. 3). This effect is the subject of the studies described in Chapter II. Aberrant declinations can be caused by rotations about a local vertical axis (Fig. 4). Aberrancy in both inclination and declination can be caused by a combination of the two previous factors, or by local tilting (Fig. 5). In some situations, tilt is readily determined if sedimentary rocks are present or if the rock unit studied is a layered volcanic sequence. But plutonic and metamorphic rocks contain little or no signature of the paleohorizontal and tilt is not known. Hence, provided that translations and rotations can be shown not to have occurred, then paleomagnetism can be used to determine tilt. This is the subject of the studies described in Chapter III.

Consider first the effect of a latitudinal change. Let D_o, I_o, θ_o and α_o be the observed magnetic declination and inclination, colatitude and circle of confidence of the direction and D_e, I_e, θ_e and α_e the same quantities obtained using data from cratonic North America. Then the poleward latitudinal displacement can be obtained by:

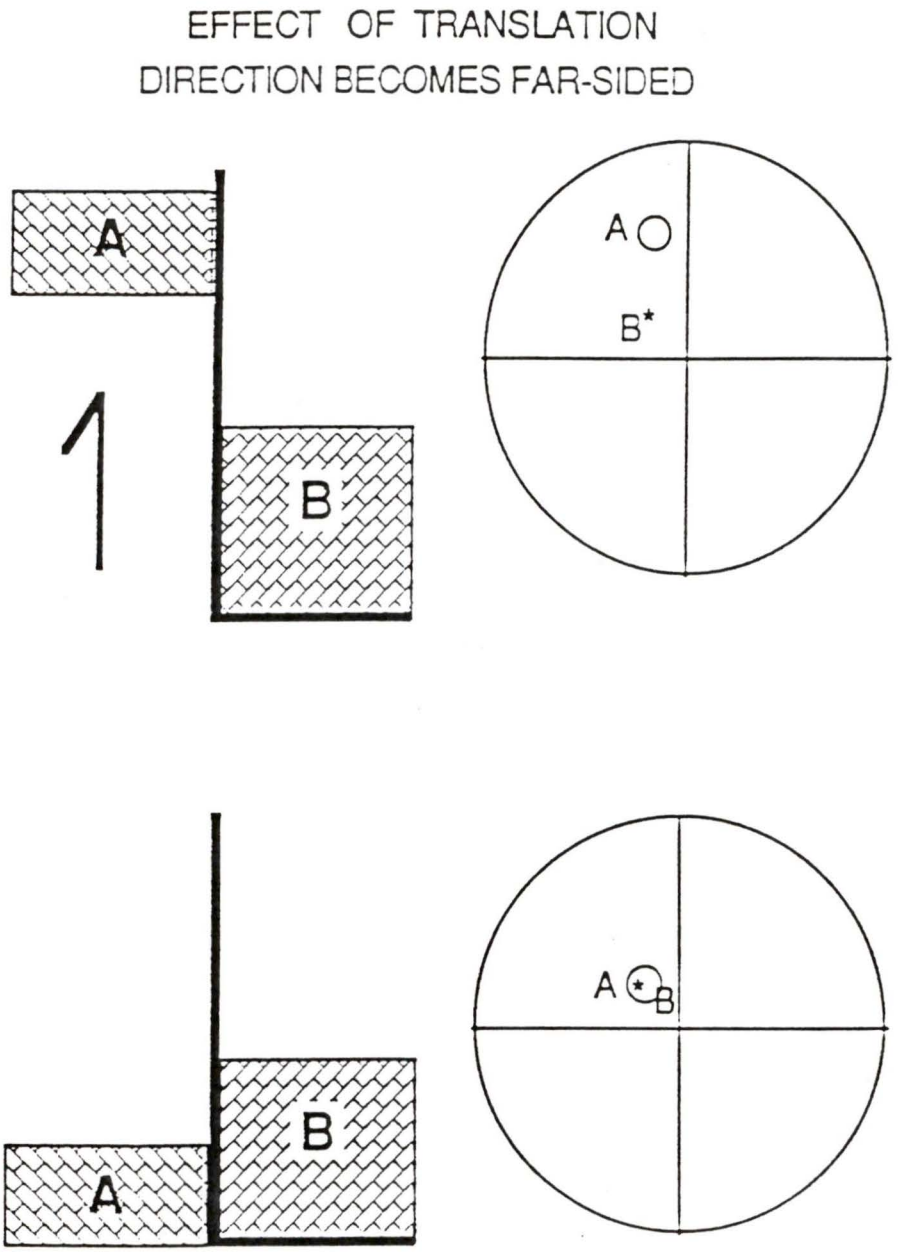

Figure 3. Effect of translation on the paleomagnetic direction

EFFECT OF ROTATION
ABOUT A VERTICAL AXIS

DIRECTION BECOMES RIGHT-HANDED

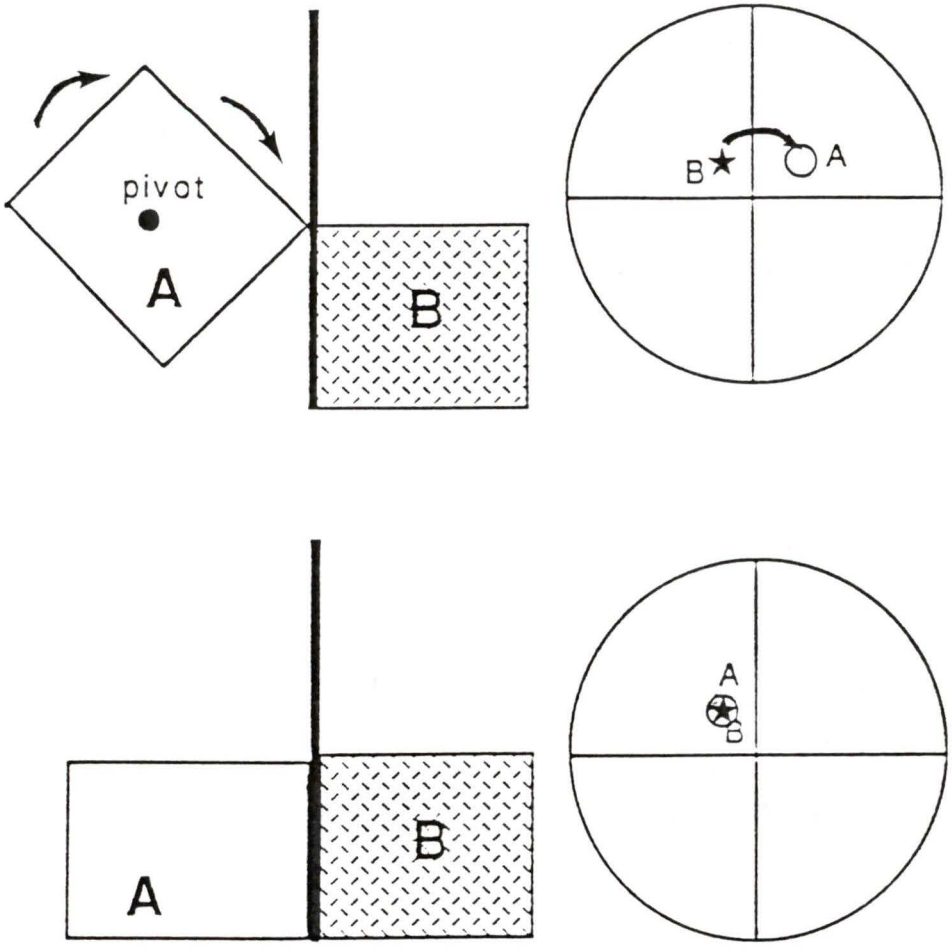

Figure 4. Effect of rotation on the paleomagnetic direction

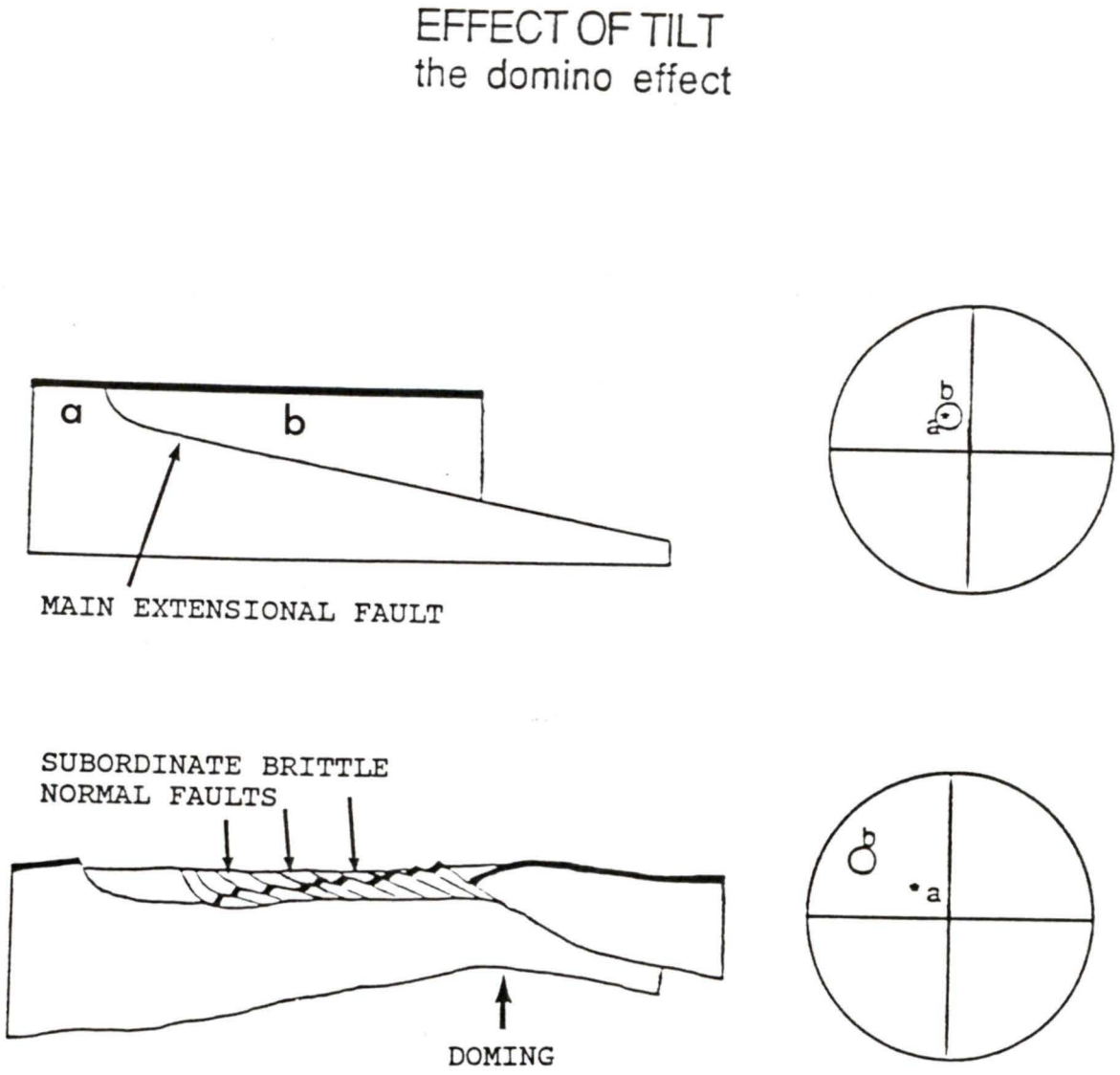

Figure 5. Effect of tilting on the paleomagnetic direction

$$d = \theta_o - \theta_e.$$

Since 2 cot θ = tan I for a geocentric axial dipole field

$$d = \cot^{-1} \frac{\tan I_o}{2} - \cot^{-1} \frac{\tan I_e}{2}$$

and the 95% confidence interval for d is

$$d = \frac{\Omega}{2} (\alpha^2_o + \alpha^2_e)$$

where Ω is the two-dimensional Gaussian correction factor (Demarest, 1983; Table 1).

The amount of rotation, R, is given by

$$R = D_e - D_o$$

and the 95% confidence interval for R is

$$R = \Omega (\Delta D_e^2 + \Delta D_o^2)$$

where

$$\Delta D_{e,o} = (\sin^{-1} (\sin \alpha_{e,o} / \sin \theta_{e,o}))/\sqrt{2}.$$

Finally, the tilt is obtained by solving the matrix equation

$$\begin{bmatrix} \cos D_e \cos I_e \\ \sin D_e \cos I_e \\ \sin I_e \end{bmatrix} = \begin{bmatrix} \cos A & \sin A & \\ -\sin A \cos BD & \cos A \cos BD & \sin BD \\ \sin A \sin BD & -\sin BD \cos A & \cos BD \end{bmatrix} \begin{bmatrix} \cos D_o \cos I_o \\ \sin D_o \sin I_o \\ \sin I_o \end{bmatrix}$$

where A and BD are the bedding down-dip azimuth and dip respectively.

Table 1

Two-dimensional

gaussian correction factor

N	Ω
2	0.70
3	0.75
4	0.76
5	0.77
6-8	0.78
9-21	0.79
22-	0.80

From Demarest (1983). N, number of sites.

Somewhat more conveniently, tilt can be determined graphically using an equal-area projection. First plot both directions as in 6(a). Then rotate until both directions lie on the same small circle. The bedding dip is given by the small circle distance between both points and the bedding down-dip azimuth is shown by the bold angle on 6(b).

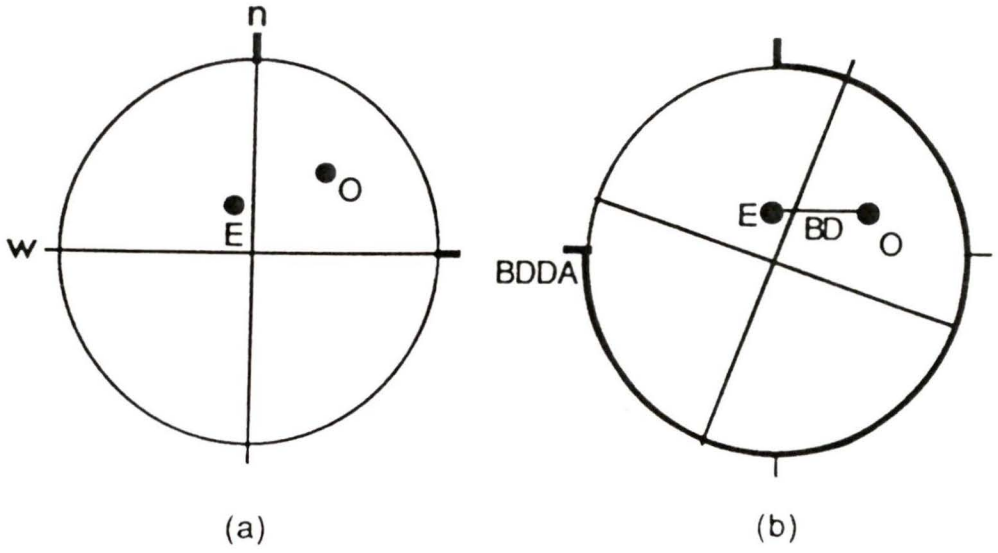

Figure 6. Finding tilt from expected and observed directions

To determine the causes of aberrancy in any particular paleomagnetic study, external evidence is needed. These evidences can come from structural geology, geochronology, stratigraphy, paleomagnetic work

on other units, etc. The general plan of my thesis, is to apply paleomagnetism to two tectonic problems in the Canadian Cordillera and compare my conclusions with independent evidence available to this date. As already noted, The first of these problems concern translation (Chapter II), the second the determination of geological tilt in high-grade metamorphic terranes (Chapter III).

CHAPTER II UPPER CRETACEOUS CARMACKS GROUP

1. *Introduction*

This is a study describing aberrant inclinations in the Yukon and northern British Columbia and their possible causes. The area in west-central Yukon and northwest British Columbia, lying east of the Denali fault and west of the Tintina-Northern Rocky Mountain Trench fault, encompasses the Yukon Crystalline and Yukon Cataclastic terranes, the Cassiar and the Cache Creek terranes, the Teslin Suture Zone (Templeman-Kluit, 1976,1981), and the Whitehorse Trough. The Whitehorse Trough forms the northern part of the Intermontane Belt (Templeman-Kluit, 1979; Tipper *et al.*, 1981). Scattered through the Whitehorse Trough are remnants of volcanic strata which are termed collectively the Carmacks group.

Large-scale motion, relative to North America, of much of the western Cordillera during Late Cretaceous and Early Tertiary time has been proposed on the grounds of stratigraphic discontinuities and paleomagnetic data (e.g. Gabrielse, 1985; Irving *et al.*, 1985). The displaced region includes the Intermontane Superterrane (I) along with Wrangellia, Alexander, and other outboard terranes referred to collectively as the Insular Superterrane (II) (Monger and Berg, 1987; Wheeler and McFeely, 1987). This large composite terrane (Superterranes I and II) has been termed "Baja British

Columbia" (Irving, 1985; Fig. 7). The main weakness in the paleomagnetic argument for displacement is that much of the data come from intrusions for which there is little or no direct attitudinal control. Hence, systematic local or regional tilting rather than translation could explain the observed aberrancies in direction (Irving, 1979; Beck *et al.*, 1981a). Also these intrusions, being mid-Cretaceous in age, precede the hypothesized northward motion of Baja British Columbia and hence provide no information on the motion itself; they record the starting position only. Since the bedding of the Carmacks group can be determined in the field, any observed aberrancy has to be caused by rotation and/or translation. Attitudes were determined by orientation of flow boundaries, colour banding or subhorizontal joints, or were obtained from existing geological maps. Data from the Carmacks group since it is Upper Cretaceous could provide an intermediate point for the displacement history of Baja British Columbia, and also provide and indirect check on the uncertainty regarding the attitudinal correction of the mid-Cretaceous intrusions.

2. *Geology*

The Carmacks group has a confusing history of nomenclature and age assignement. In west-central Yukon, Upper Cretaceous to lower Cenozoic volcanic strata were

SIMPLIFIED TERRANE MAP OF YUKON-BRITISH COLUMBIA

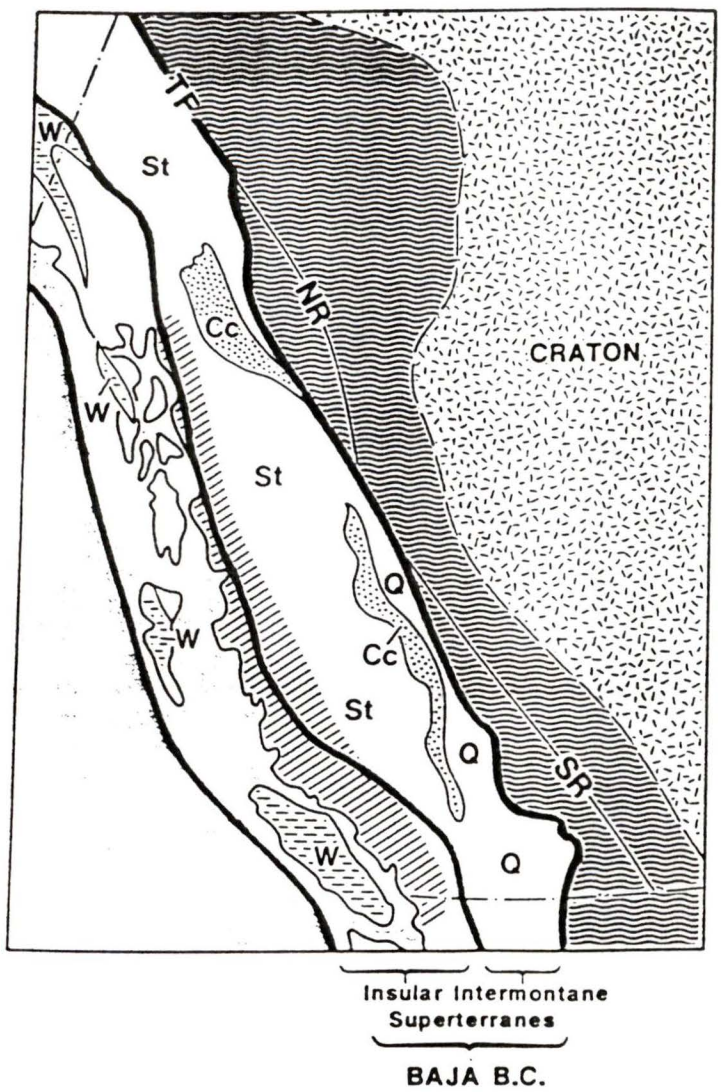

Figure 7. Map showing the main tectonic features of the Canadian Cordillera. Terranes: W, Wrangellia; St, Stikinia; Cc, Cache Creek; Q, Quesnelllia. TF, Tintina Fault; NR and SR, Northern and Southern Rocky Mountain Trench. From Irving and Wynne (1988).

called the Carmacks group by Templeman-Kluit (1974, 1978, 1980), while in southern Yukon and northwest British Columbia similar rocks were called the Hutshi group by Wheeler (1961) and Bultman (1979). Bostock (1936) correlated the Hutshi group with volcanic rocks in the Carmacks district, which he named Mount Nansen. Geochronological work by Grond *et al.* (1984) demonstrated that the Carmacks, Mount Nansen and Hutshi groups were contamporaneous. In order to simplify the nomenclature, Wheeler and McFeely (1987) regrouped under the name Carmacks all Upper Cretaceous volcanic strata in Yukon and northwest British Columbia.

Grond *et. al* (1984) obtained five K-Ar whole rock and mineral dates for andesites and basalts collected from the Miners Range region and from Carmacks (Fig. 8). They also calculated a Rb-Sr isochron (using basalt, andesite, and rhyolite) for samples collected on the summit of Table Mountain west of Atlin, British Columbia (Table 2). The average of these six radiometric ages is 70.4 +/- 2.4 Ma, i.e. Late Cretaceous.

Sampling localities

Sampling has been made in the Carmacks, Miners Range, and Atlin Lake regions, for which sufficient geochronologic and geologic information is available (Fig. 8). The geology of the sampling localities is summarized

MAP OF THE SAMPLING AREA

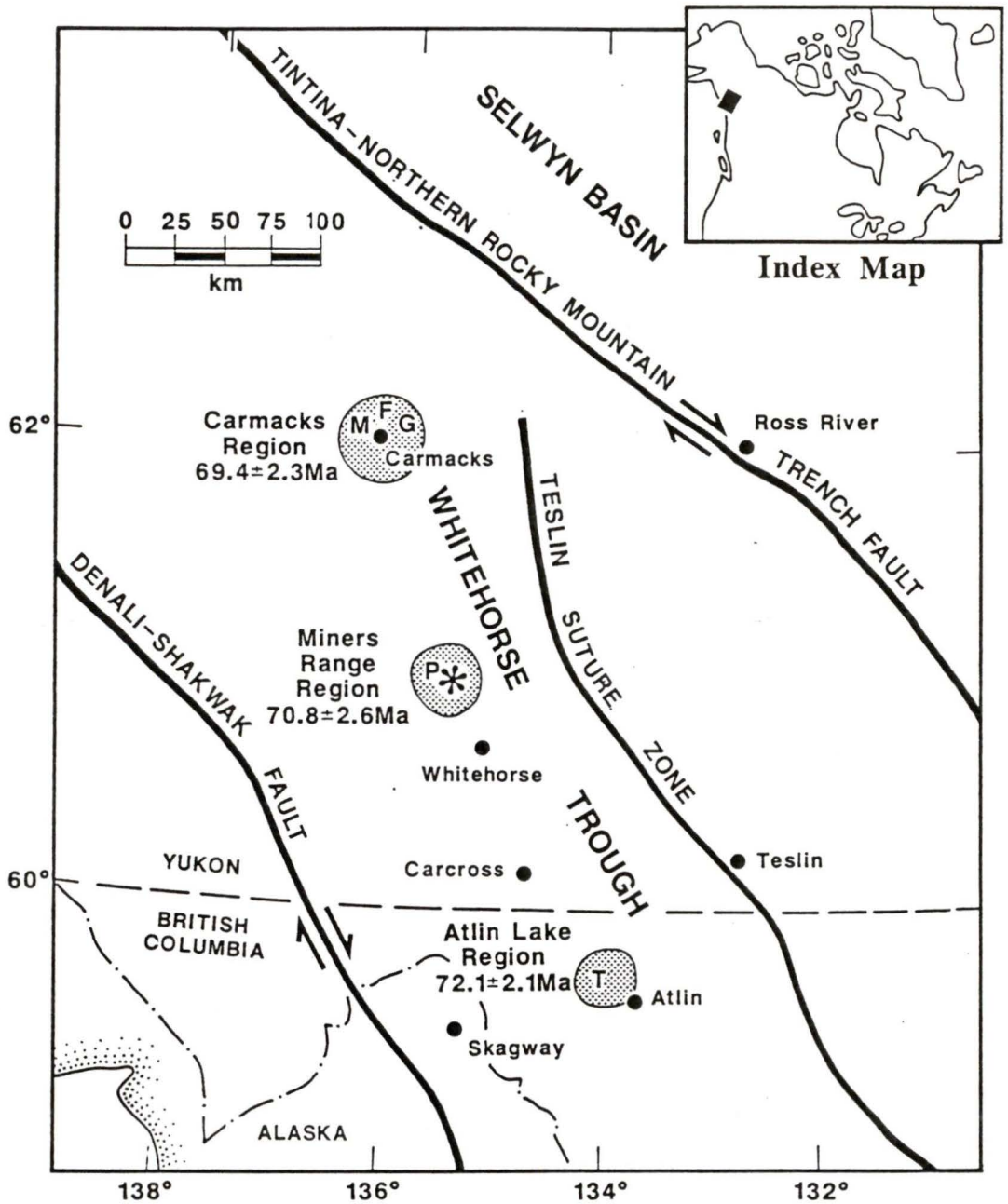

Figure 8. Map of west-central Yukon and northwest British Columbia showing locations and ages of Carmacks, Miners Range and Atlin Lake regions. Sampling sections: M, Miller's Ridge; F, Five-Finger Mountain; G, Glenlyon; P, Pilot Mountain; T, Table Mountain. Star denotes mean site coordinates.

Table 2

Compilation of isotopic dates for Carmacks group

Region	Lat, Long (°N, °E)	method	Age Ma +/- σ
Carmacks	62.07, 223.59	K/Ar wr	73.1+/-2.5
Carmacks	62.07, 224.05	K/Ar bi	68.0+/-2.2
Carmacks	61.97, 223.78	K/Ar wr	67.9+/-2.3
	Region average		69.4+/-2.3
Miners Range	61.17, 223.78	K/Ar wr	72.4+/-2.5
Miners Range	61.15, 224.38	K/Ar pl	69.1+/-2.6
	Region average		70.8+/-2.6
Atlin Lake	59.63, 226.05	Rb/Sr isochron	72.4+/-2.1
	GRAND AVERAGE		70.4+/-2.4
	(n = 6)		

Data obtained by Grond *et al.* (1984), University of British Columbia Geochronology Laboratory. Rb/Sr isochron obtained from rhyolite, andesite, trachybasalt and alkalic basalt. Averaging procedures from Darlymple and Lamphere (1969). K analyses were made by atomic absorption and Ar analyses by isotope dilution. Rb and Sr proportions were determined by X-ray fluorescence analysis of fused disks.

in Table 3. These informations come mainly from field observations completed with different reports and theses (Bostock, 1936; Aitken, 1959; Campbell, 1967; Templeman-Kluit, 1974, 1978, 1980, 1984; Bultman, 1979; Churchill, 1980; Grond, 1980).

Carmacks region

Samples were collected from three sections in the Carmacks region. The sites which yielded coherent data are listed in stratigraphic order in Table 3, the oldest at the bottom. The Glenlyon section is completely fault-bounded, and is separated from the other sections by tightly-folded Jura-Cretaceous strata. It comprises sheared, vesicular andesite intercalated with epiclastic breccia and immature sandstone. Alteration appears pervasive, probably due to the extensive fracturing and fluid circulation. It is therefore not surprising that only one site yielded consistent paleomagnetic data.

The Five-Finger Mountain section consists of blocky-jointed, porphyritic basalt lava flows. The bedding attitude was extrapolated from mapped attitudes of the nearest basalt outcrops located west of Five-Finger Mountain, on the west side of the Braeburn fault (Templeman-Kluit, 1984). The Miller's Ridge summit section comprises massive, flat-lying basalt. Sampling

Table 3

Collecting sites, Carmacks group

Site	rock type	Lat, Long (°N, °E)	strat. dist.	attitude (BDDA/BD)	Rel. att.
MILLER'S RIDGE SUMMIT SECTION, CARMACKS REGION					
KCG-15	basalt	62.17, 223.33	150	flat	X
KCG-12	basalt	62.17, 223.33	150	flat	X
KCG-14	basalt	62.17, 223.33	120	flat	X
KCG-13	basalt	62.17, 223.33	30	flat	X
KCG-11	basalt	62.17, 223.33	0	flat	X
FIVE-FINGER MOUNTAIN SECTION, CARMACKS REGION					
KCG-10	basalt	62.16, 223.74	230	270/5	Z
KCG-09	basalt	62.16, 223.74	0	270/5	Z
GLENLYON SECTION, CARMACKS REGION					
KCG-03	andesite	62.06, 224.05	0	50/20	Y
PILOT MOUNTAIN SECTION, MINERS RANGE REGION					
KCG-17	andesite	61.03, 224.50	150	341/10	Y
KCG-18	andesite	61.03, 224.50	90	341/10	Y
KCG-20	andesite	61.03, 224.50	50	341/10	Y
KCG-21	andesite	61.03, 224.50	30	341/10	Y
KCG-19	andesite	61.03, 114.50	0	341/10	Y

Table 3 (continued)

Site	rock type	Lat, Long (°N, °E)	strat. dist.	attitude (BDDA/BD)	Rel. att.
TABLE MOUNTAIN SECTION, ATLIN LAKE REGION					
KCG-35	andesite	59.64, 226.08	900	240/13	Y
KCG-34	andesite	59.64, 226.08	890	240/13	Y
KCG-38	andesite	59.64, 226.08	770	240/13	Y
KCG-37	andesite	59.64, 226.08	750	240/13	Y
KCG-33	and. brecc	59.63, 226.08	0	240/13	Y

Approximate up-section distances measured from the bottom. Bedding attitudes are given by bedding down-dip azimuth (BDDA) and dip (BD). Reliability : X, good, attitude determined at the site; Y, reasonable, attitude from geologic maps and distant sightings; Z, poor, inferred from sparse evidence on geologic maps.

covered about 150 m of stratigraphic section.

Miners Range region

The Pilot Mountain section consists of massive- to columnar-jointed porphyritic andesite containing phenocrysts of plagioclase and hornblende. The section dips 10° to the northwest. Sampling spanned about 150 m stratigraphically.

Atlin Lake region

The Table Mountain region comprises mainly porphyritic andesite, with subordinant varicoloured basalt, dacite, and rhyolitic tuff. The bedding attitude is from Aitken (1959), who observed a 10 to 15° southwest dip of the volcanic strata. Sampling has been made at the summit of Table Mountain, west of Atlin.

Sampling methods

Using portable drilling equipment, 201 oriented cores from 27 sites were collected. The core down-dip azimuth was determined using a magnetic compass and checked with a sun compass where possible and by distant sightings otherwise. The core dip was measured with an orienting tube. The cores were then cut in cylindrical specimens (usually two per core), of one inch diameter by one inch length.

3.*Remanent magnetization*

Methods

i.*Measurements*

Magnetization measurements were made on a Schonstedt SSM-1 spinner magnetometer coupled to an IBM PC. The rock specimen is spun in front of a fluxgate. This generates a magnetic field that makes the fluxgate generate alternating currents. Using a digital Fourier Transform, the current is decomposed into two components, providing two measurements for each face of the specimen, i.e. 4 independent measurements for the x, y, and z components of the magnetization vector. A data acquisition system stores these data into the computer's memory for statistical processing.

ii.*Fisher's statistics*

Let X_i, Y_i, Z_i be the measurements of the x, y, and z components of the magnetization vector. Their respective lengths V_i are

$$V_i^2 = X_i^2 + Y_i^2 + Z_i^2$$

and their direction cosines are

$$l_i = \frac{X_i}{V_i} \qquad m_i = \frac{Y_i}{V_i} \qquad n_i = \frac{Z_i}{V_i} \quad .$$

Fisher (1953) showed that the best estimate (l,m,n) of the true mean direction is

$$l = \frac{\Sigma\, l_i}{R} \qquad m = \frac{\Sigma\, m_i}{R} \qquad n = \frac{\Sigma\, m_i}{R}$$

where $R^2 = (\Sigma l_i)^2 + (\Sigma m_i)^2 + (\Sigma n_i)^2$.

The declination and inclination of the mean are

$$D = \tan^{-1} (\Sigma m_i / \Sigma l_i)$$

$$I = \sin^{-1} (\Sigma n_i / R).$$

He also showed that the best estimate of the precision parameter k is

$$k = (N - 1)/(N - R).$$

The approximate circular standard deviation (θ_{63}) is given by

$$\theta_{63} = 81/\sqrt{k} \quad \text{degrees,}$$

which is the radius of the circle whose centre is the true mean and which contains 63% of the individual directions. The standard error of the mean (α_{63}) and the circle of 95% confidence are given by

$$\alpha_{63} = 81/\sqrt{(kN)} \quad \text{degrees and}$$

$$\alpha_{95} = 140/\sqrt{(kN)} \quad \text{degrees.}$$

These are the radii of the circles centered on the mean direction and which contain the true direction at 63 and 95% levels of confidence.

This statistical technique can be applied to sets of directions for calculating a site-mean direction (1-2 analysis), then to mean-site directions for calculating a mean direction for the whole rock sequence (2-3 analysis). Converting directions (D, I) into direction cosines can be done using the spherical coordinate relationships

$$l_i = \cos I_i \quad \cos D_i$$

$$m_i = \cos I_i \quad \sin D_i$$

$$n_i = \sin I_i .$$

iii.*Demagnetization techniques*

Specimens were demagnetized by alternating fields (AF), using a Schonstedt GSD-5 tumbler-demagnetizer. The specimen is put into a coil which is driven by an AC power supply. This generates an alternating field which is then slowly decreased. All the magnetic grains in the specimen which have a coercivity equal to or smaller than the peak magnetic field in the coil will have their magnetizations aligned parallel to the field. As the field falls the grains will become remagnetized, but because the field is alternating and because the specimen is tumbled, their directions will be randomized (Creer, 1959). Only the magnetization of the grains with higher coercivity will continue to contribute to the total magnetization of the specimen. This is repeated with increasing peak field up to the maximum value available in the laboratory, 100 mT. For most of the sites, the optimum cleaning field was 40 mT, except for site 03 (20 mT), for site 11 (30 mT) and sites 09, 10 and 18 (60 mT).

Some specimens were demagnetized thermally following the method described by Thellier (1937), using a

Schonstedt shielded furnace. The specimen is heated up to a certain temperature T_o. All the magnetic grains with unblocking temperatures lower than T_o will lose their magnetization. The specimen is then cooled in field-free space, so that the magnetization acquired by all these grains will essentially be random. Only the high unblocking temperatures will continue to contribute to the total magnetization of the specimen. This is repeated with increasing temperatures until all magnetization is destroyed, usually up to 650°C.

The magnetization directions observed at each of these steps can then be plotted on an equal-area projection (Figs. 9(a) to 11(a)). In some instances, an end-point is reached when the demagnetization at higher steps does not affect the magnetization direction. The directions and their intensities can be combined to calculate the projections of the magnetization vector on different planes (Figs. 9(b) to 11(b)). These are called orthogonal plots (Zijderveld, 1967). If the projections of the magnetization vector between consecutive demagnetization steps plot on a line, this line defines a component of the total magnetization. This method can show if one or more components are present.

The ratios of the intensity of the magnetization vector at any demagnetization step to the intensity of the NRM vector are also plotted (Figs. 9(c) to 11(c)).

They give an indication of the stability of the magnetization and sometimes the nature of the magnetic carriers. For example if the intensity vanishes around 580°C, the magnetization is most probably carried by magnetite grains.

Types of magnetization

The magnetizations of specimens have been grouped into three categories - A, B and C according to their behaviour during demagnetization. A-type magnetizations have orthogonal plots showing linear decay to the origin, at temperatures above 300°C, after removal of a subordinate soft magnetization probably viscous remanent magnetization (VRM) approximately parallel to the present earth's field (PEF), or at alternating fields, above 20 mT after removal of a soft magnetization presumed to be an isothermal remanent magnetization (IRM) caused by lightning. These decay lines define the principal magnetization whose direction has been obtained by selecting a cleaning temperature or field along the lines, since A-type magnetizations have excellent end-points for both AF and thermal demagnetizations. An example of A-type magnetization demagnetized by AF is shown in Fig. 9. Although there is a strong component with low coercivity (10 mT), probably caused by lightning, a stable high coercivity component is isolated by 60 mT. An example of ideal single component

Table 4

Quality of paleomagnetic data, Carmacks group

Site	A, B, C	Site	A, B, C
MILLER'S RIDGE		FIVE-FINGER	
KCG-15	9, 3, 3	KCG-10	6, 1, 0
KCG-12	6, 3, 4	KCG-09	5, 1, 0
KCG-14	7, 0, 2		
KCG-13	11, 1, 0	GLENLYON	
KCG-11	2, 3, 8	KCG-03	2, 5, 5
PILOT MOUNTAIN		ATLIN LAKE	
KCG-17	4, 7, 0	KCG-35	9, 1, 0
KCG-18	8, 5, 4	KCG-34	9, 2, 0
KCG-20	6, 2, 3	KCG-38	3, 2, 1
KCG-21	3, 2, 6	KCG-37	9, 1 ,1
KCG-19	9, 1, 0	KCG-33	5, 3, 1

Quality labels A, B, and C described in text.

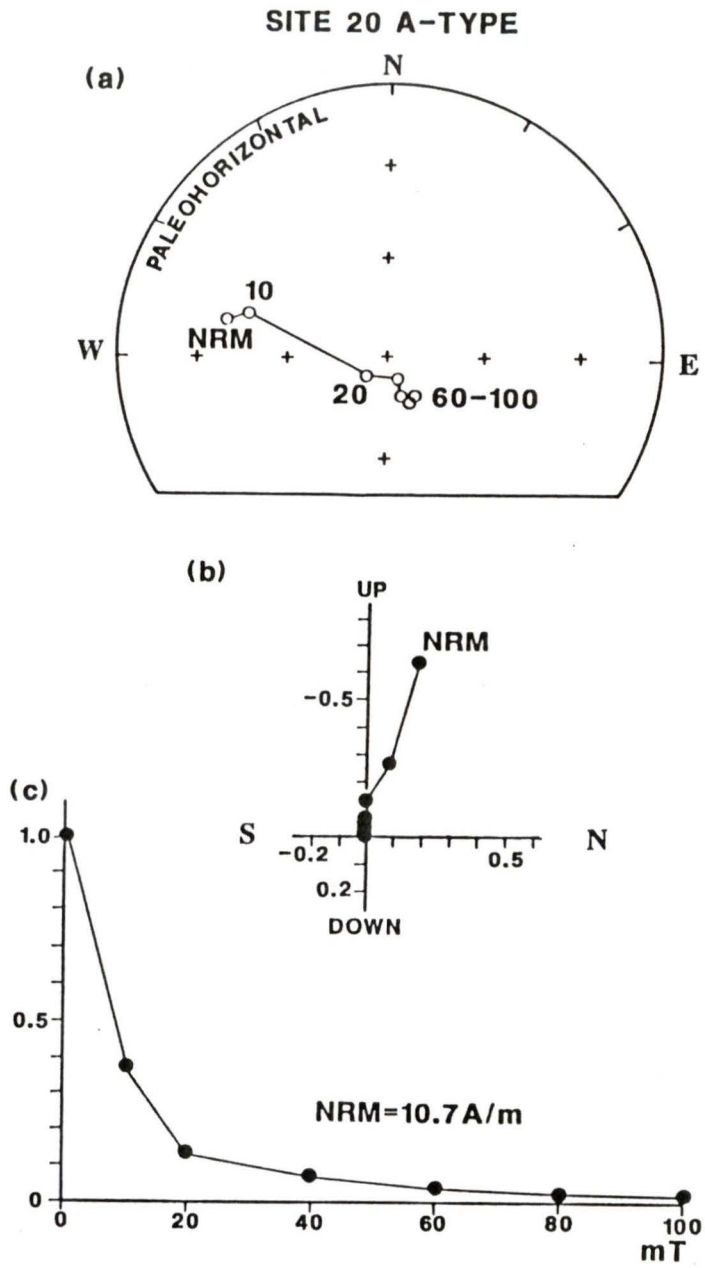

Figure 9. AF demagnetization of A-type magnetization. Equal-area projection (a), orthogonal plot (b) and decay of normalized intensity (c). In equal-area plots, solid (open) circles denote positive (negative) inclination. In this example, the original TRM is partially overprinted by an IRM.

A-type magnetization with a narrow range of unblocking temperatures (550-580°C) is shown in Fig. 10. This is characteristic of almost pure magnetite. In fact, in most of the specimens studied here, low-Ti titano-magnetite appears to be the main carrier of natural remanent magnetization (NRM).

B-type magnetizations, like A-type, have orthogonal plots which show linear decay. Sometimes the decay lines pass close to the origin and there is a crude end-point (Figs. 11 and 22). The observed points are distributed more widely about the line than in A-type magnetization, thus the line is less well defined. In other instances, the decay lines do not pass to the origin so that a very hard magnetization is present (Fig. 23). The hard magnetization is small in magnitude compared to the principal magnetization defined by the lines. An example of thermal demagnetization of a specimen with B-type magnetization is shown in Fig. 11. The specimen yields components with unblocking temperatures distributed from 300°C up to 500°C and with irregular directions as shown by the orthogonal plot. However, above 500°C, the decay is linear to the origin and the directions are well clustered.

C-type magnetizations have plots which do not suggest

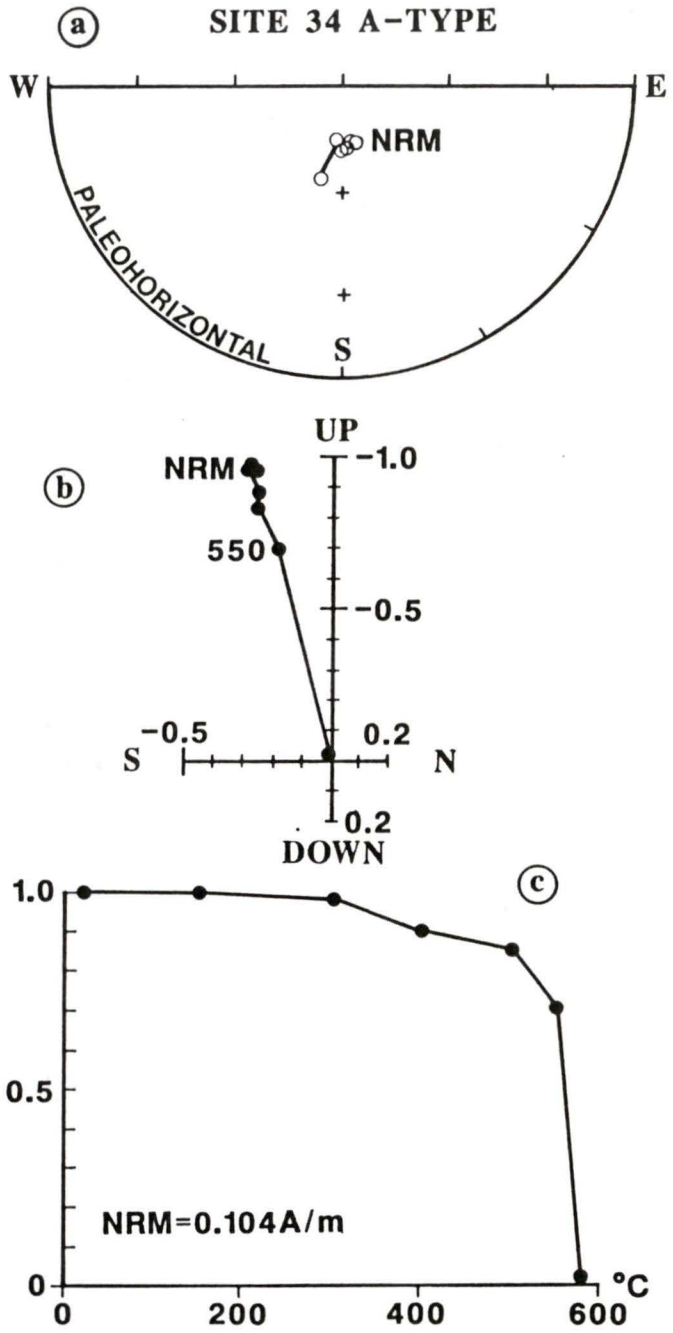

Figure 10. Thermal demagnetization of A-type magnetization. Note the discrete unblocking temperatures indicated by the almost perfect magnetite "shoulder".

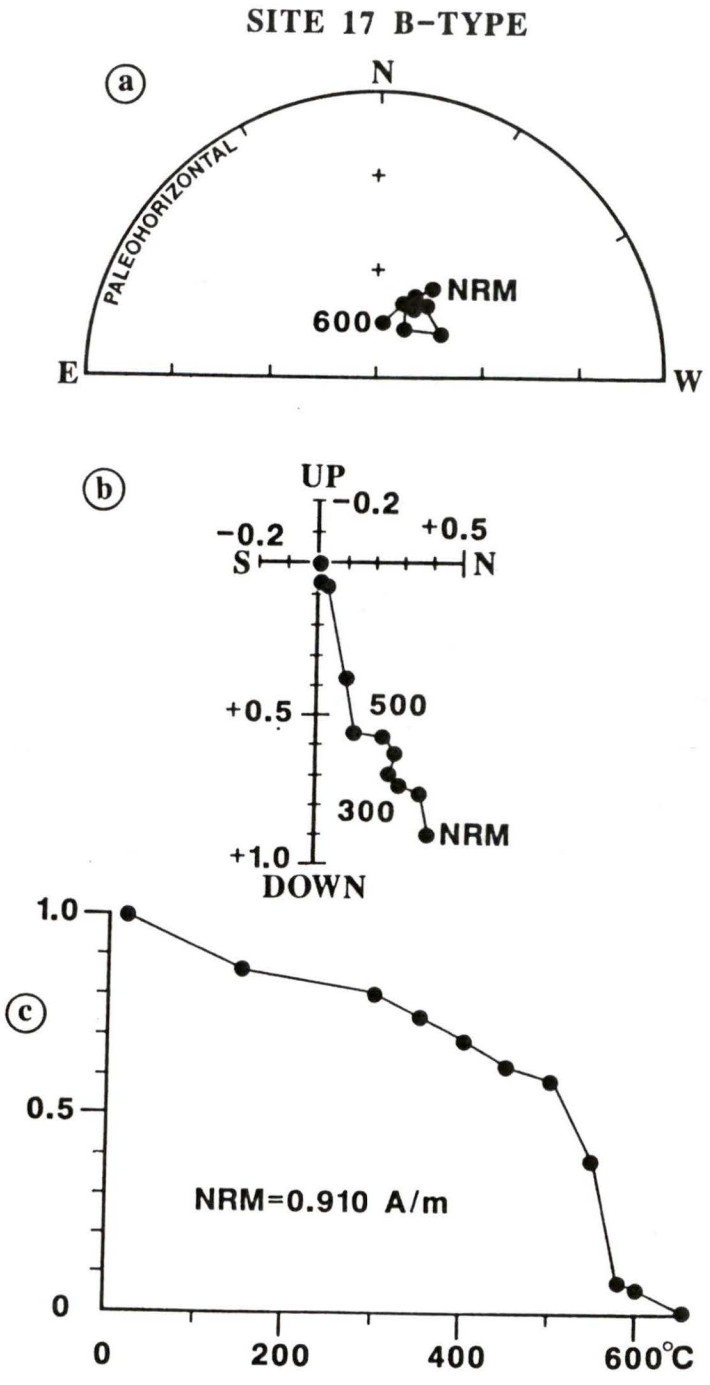

Figure 11. Thermal demagnetization of B-type magnetization. Unblocking temperatures are more distributed than those in figure 10.

any linear decay, and have no end-point. Included here are magnetizations with directions farther than two standard deviations from the site-mean direction. Some of these aberrant magnetizations have weak intensities ($\approx 10^{-2}$ A/m), and remanent directions almost parallel to the PEF. Others have strong intensities ($\approx$10 A/m) and good within specimen precisions. However, neither AF nor thermal cleaning produced a change in direction, suggesting that a "hard" IRM has replaced the original thermoremanent magnetization (TRM).

Laboratory tests for magnetic properties

In order to determine the cause of this variable behaviour, certain experiments were carried out : IRM and low-field TRM acquisition and AF decay, and anisotropy of remanent magnetization. Typical IRM acquisition curves are shown in Fig. 12. The saturating fields range from 0.14 to 0.22 T. These specimens were then demagnetized by AF up to 100 mT (Fig. 13). In addition, specimens were given low-field TRM, and then were demagnetized in alternating fields. Normalized intensity decay curves for NRM, IRM and TRM are shown in Fig. 13 for two specimens. The specimen from site 03 (andesite) exhibits typical multi-domain grain behaviour, because the saturation IRM is more stable than the low-field TRM (Lowrie and Fuller, 1971). This is also

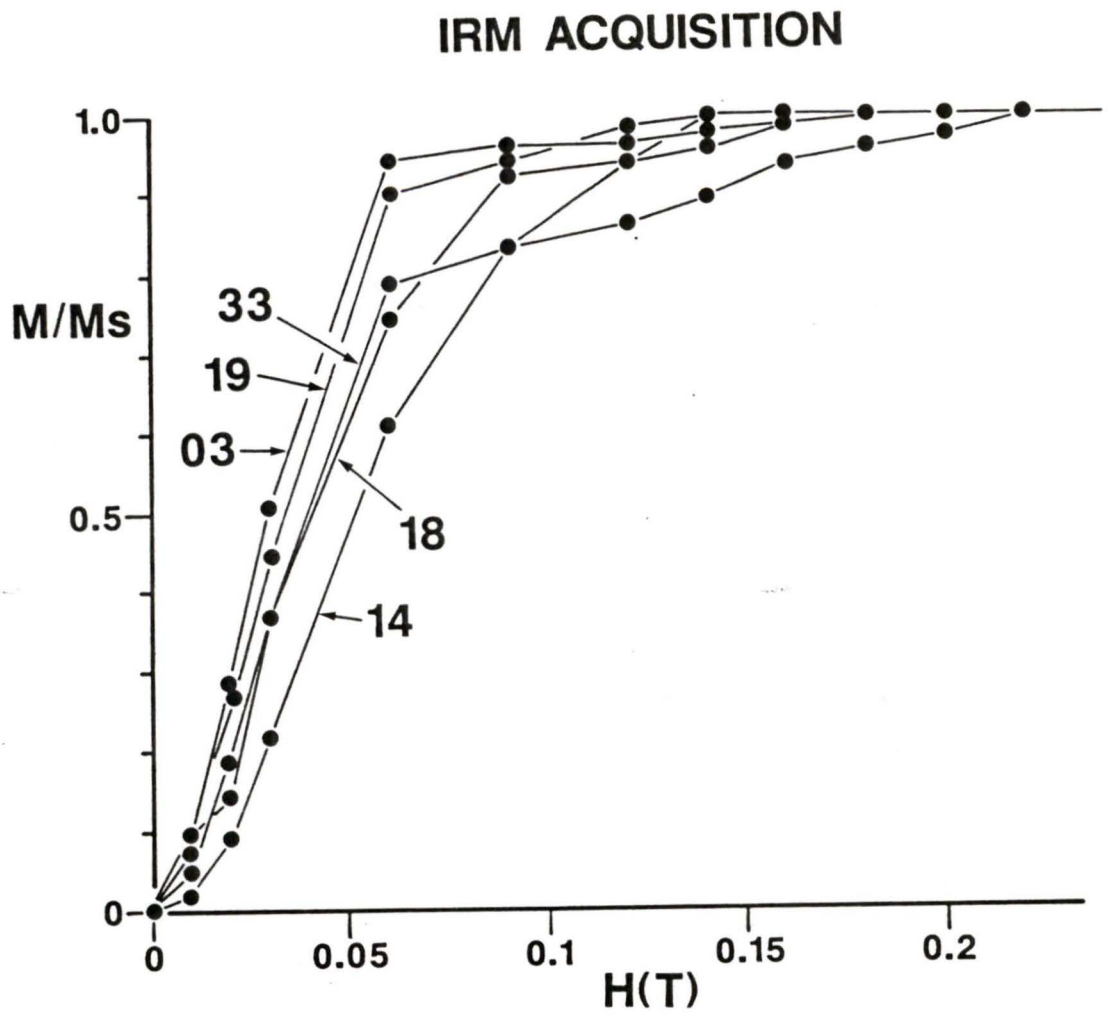

Figure 12. Normalized IRM acquisition curves. Saturation remanent magnetizations are as follows in A/m: site 03, intensity 184; 14, 372; 18, 221; 19, 122; and 33, 49.

LOWRIE AND FULLER (1971) TEST

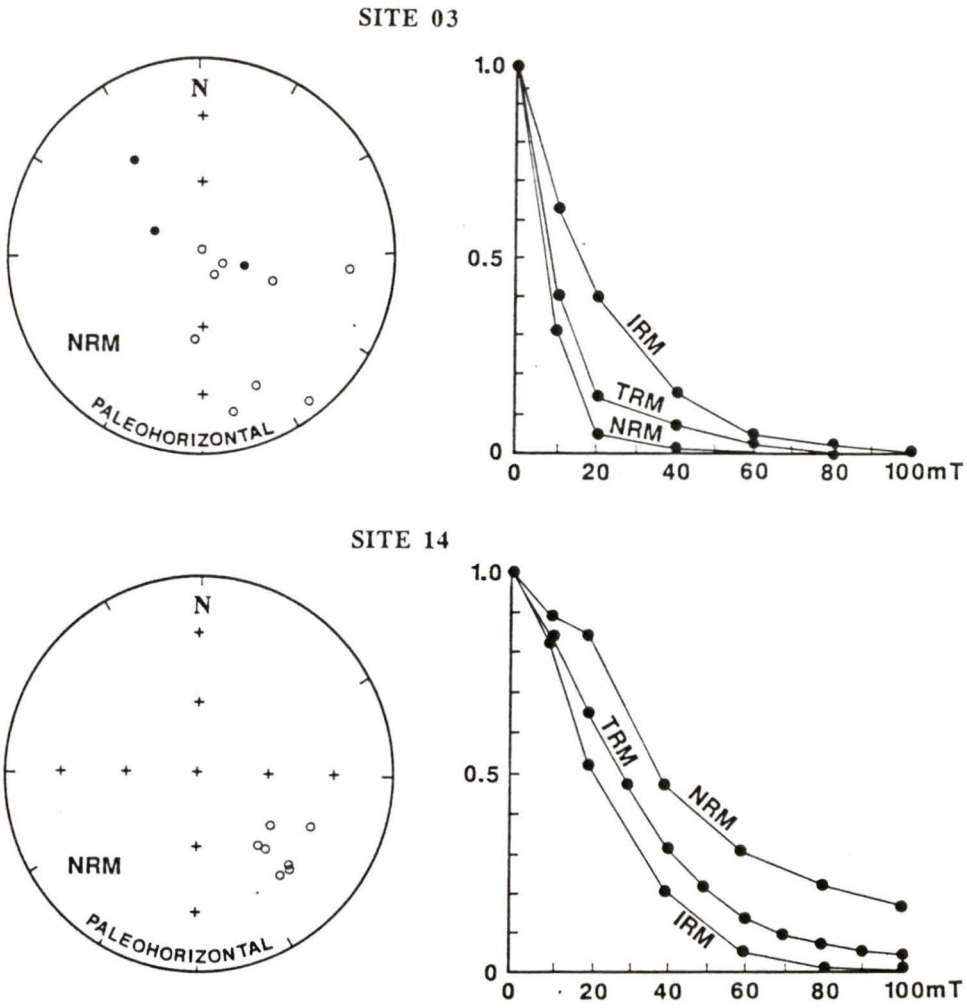

Figure 13. Site-mean NRMs and comparison of AF demagnetization of NRM, IRM, and TRM for one specimen from each site. Site 03, multi-domain behaviour; site 14, single-domain behaviour.

supported by the large sizes (200-300 μm) of the magnetic carriers as shown in the reflection microscope photograph (Fig 14). The NRMs for site 03 are very scattered because the original TRM has decayed rapidly and the specimens acquired soft randomly distributed magnetizations. Most of the magnetizations from site 03 are B- or C-type (10/12 specimens). The specimen from site 14 (basalt) exhibits typical single-domain grain behaviour, the low-field TRM being more stable than the saturation IRM. The sizes of the magnetic carriers (5-25 μm) indicate that they are slightly larger than the typical single-domain size ($<$ 3 μm) for magnetite grains, i.e. pseudo single-domain. Except for two specimens with magnetizations directed toward the west and which are associated with lightning strikes, the NRMs from site 14 show good cluster because the original TRM is very stable. Specimens from site 14 show mainly A-type magnetizations (7/9 specimens). Therefore A- and C-type magnetizations are related to single-domain and multi-domain magnetic carriers respectively. B-type magnetizations are probably related to magnetic carriers showing intermediate behaviour.

To test the possibility of inclination error due to preferred alignement of the grains during laminar flow of the lava, two experiments of IRM and TRM acquisition

PHOTOMICROGRAPHS OF THIN SECTIONS

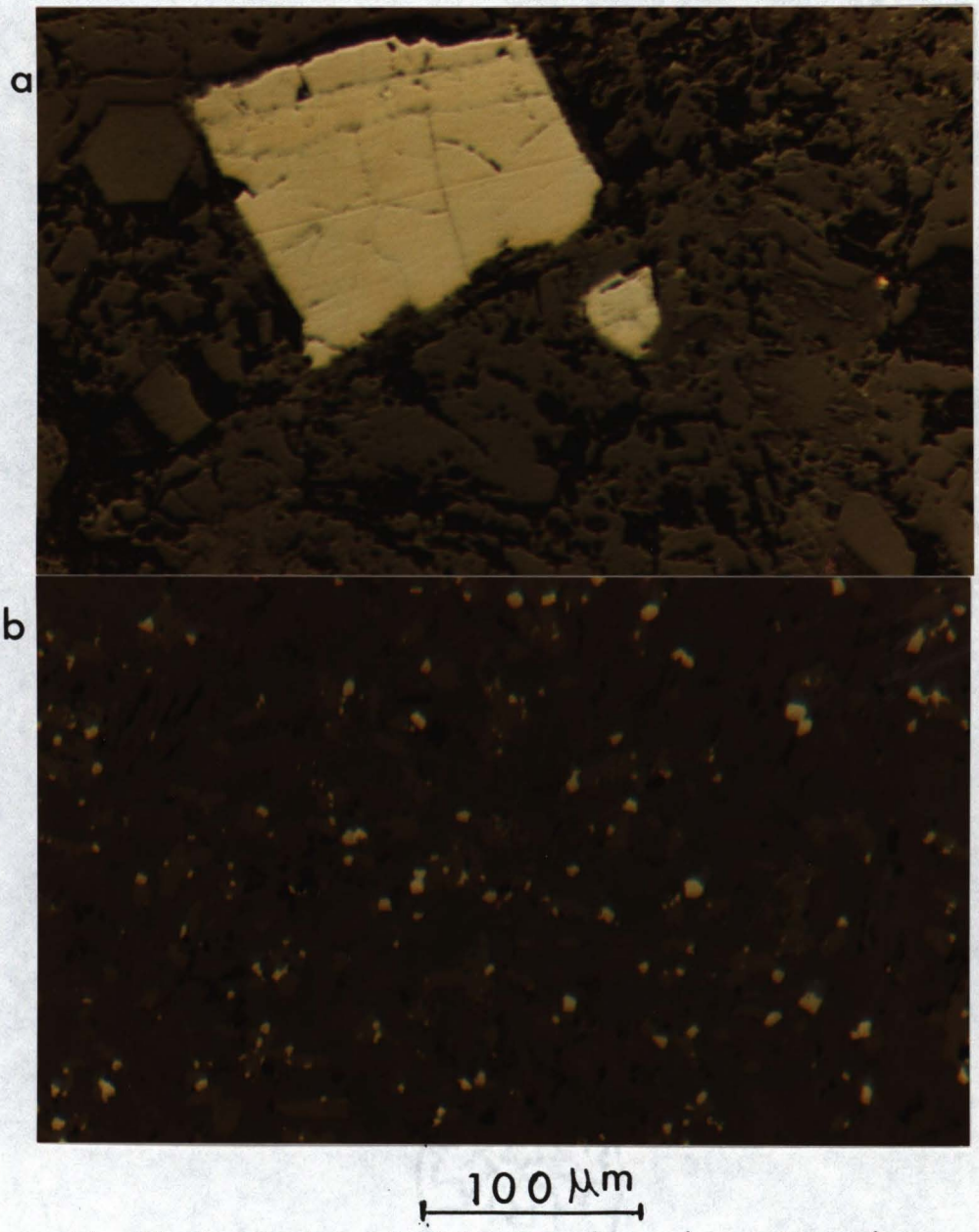

Figure 14. Photographs of thin sections in reflection microscopy. (a) sample from site 03; (b) from site 14.

were made. Eight specimens were placed in a magnetic field of 0.25 T coaxial to the specimens. The magnetizations were measured before and after demagnetization in alternating fields of 25 mT. The companion specimens were heated to 700°C and then cooled in a magnetic field of 10^{-4} T coaxial to the specimens. Magnetizations were measured before and after thermal cleaning at 500°C. The observed inclinations before and after both AF and thermal demagnetization differed by no more than 0.9° from the direction of the applied field (Table 5). Hence it is improbable that the observed specimen directions are significantly affected by anisotropy.

4. *Analysis*

Mean direction and paleopole

All the specimens showing C-type magnetizations have been omitted from the analysis. Directions of the 156 remaining specimens were used to calculate 18 site-mean directions (Fig. 15, Table 6). After the two normal polarity sites are inverted through the origin, the mean direction, giving sites unit weight, is D = 177.5°, I = -73.3°, α_{95} = 6.7° with the Fisher (1953) precision parameter k = 28. After tilt correction the mean direction becomes D = 166.7°, I = -71.4°, α_{95} = 4.8° and k = 53. The increase in k obtained upon unfolding is significant, the

Table 5

Inclinations of synthetic magnetizations

	I	α^{o}_{95}	k
IRM (0.25 T)	89.7	1.8	949
IRM after 25 mT AF demag.	89.7	4.9	131
TRM (10^{-4} T)	89.5	3.3	285
TRM after 500°C demag	89.1	5.1	112

Averages of 8 specimens. Applied field coaxial with cylindrical specimens.

Table 6

Paleomagnetic data, Carmacks group

Site	n, s, s'	$D°_H, I°_H$	$D°_B, I°_B$	k	α_{95}	Pole (λ, φ)
MILLER'S RIDGE SUMMIT, CARMACKS REGION						
KCG-15	8,15,12	179,-68	179,-68	136	4	79, 48
KCG-12	8,13, 9	173,-61	173,-61	19	12	70, 59
KCG-14	6, 9, 7	165,-69	165,-69	186	4	78, 91
KCG-13	8,12,12	168,-79	168,-79	57	6	82, 189
KCG-11	8,13,15	175,-65	175,-65	46	11	74, 57
FIVE-FINGER MOUNTAIN SECTION, CARMACKS REGION						
KCG-10	6, 7, 7	206,-60	197,-62	392	3	68, 8
KCG-09	5, 6, 6	139,-78	124,-74	540	3	64, 156
GLENLYON SECTION, CARMACKS REGION						
KCG-03	9,12, 7	121,-71	176,-68	63	8	78, 58
PILOT MOUNTAIN SECTION, MINERS RANGE REGION						
KCG-17	7,11,11	60, 86	1, 79	56	6	83, 227
KCG-18	9,17,13	40, 80	11, 73	18	10	84, 338
KCG-20	7,11, 8	136,-83	151,-73	42	9	75, 140
KCG-21	8,11, 5	106,-63	119,-57	30	14	46, 131
KCG-19	8,10,10	6,-79	73,-86	98	5	58, 210

Table 6 (continued)

Site	n, s, s'	$D°_H, I°_H$	$D°_B, I°_B$	k	α_{95}	Pole (λ, φ)
TABLE MOUNTAIN SECTION, ATLIN LAKE REGION						
KCG-35	7,10,10	182,-65	152,-69	102	5	73, 124
KCG-34	7,11,11	189,-63	162,-69	19	11	78, 110
KCG-38	6, 6, 5	211,-72	170,-81	69	9	77, 212
KCG-37	7,11,10	195,-60	173,-67	294	3	80, 73
KCG-33	6, 9, 8	199,-51	185,-60	16	14	71, 34

n, number of cores collected; s, number of specimens; s', number of specimens used in calculating site-mean directions; $D°$, $I°$, declination and inclination of the mean direction with respect to horizontal (H) and bedding (B); k, estimate of Fisher (1953) precision parameter; α_{95}, half-angle of cone of 95% confidence; λ, φ, latitude (°N) and longitude (°E) of paleopole.

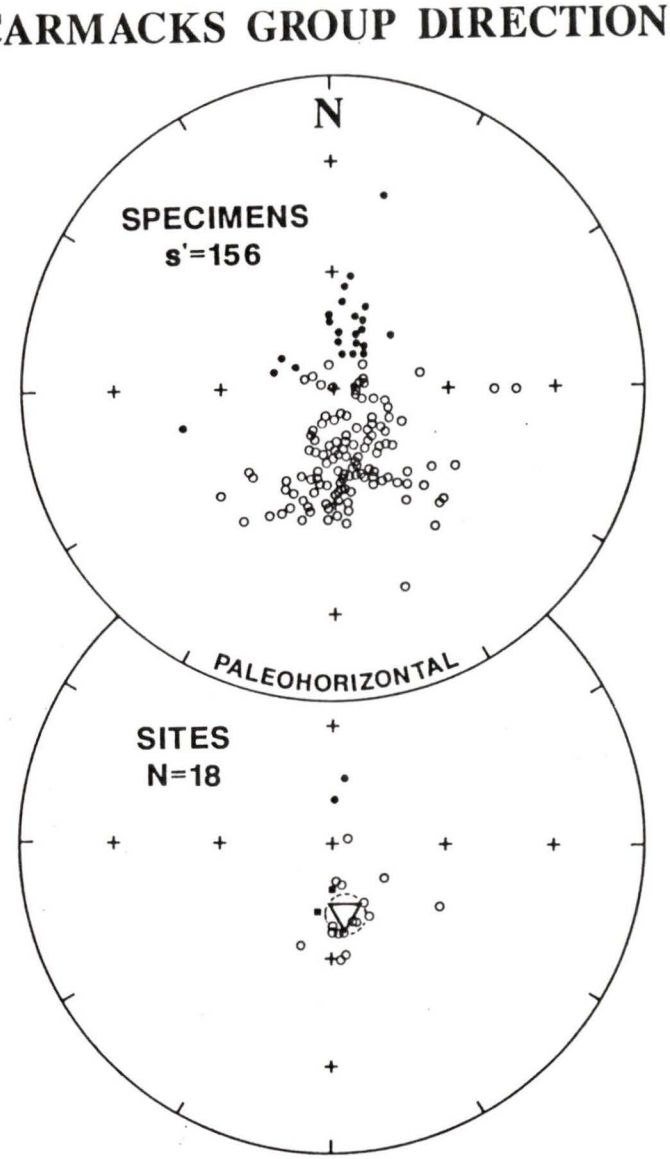

Figure 15. Directions of stable remanent magnetization. Triangle denotes mean of 18 site-mean directions. Dashed circle is cone at 95% confidence. Squares indicate directions of normal polarity sites inverted through the origin.

data passing the fold tests of Watson (1956) and McFadden and Jones (1981) at more than 95% confidence.

- Watson's test:

$$\frac{k' \text{ after tilt correction}}{k \text{ before tilt correction}} = \frac{53}{28} = 1.893$$

for N= 18 sites, the critical value for the ratio of ks at 95% confidence is 1.78 (McElhinny, 1964).

Conclusion : the fold test is significant at 95% confidence, i.e. the magnetization has been acquired before tilt.

-Mcfadden and Jones test: The distribution is divided in limbs to take account of the disparities between the different sampling areas (McFadden and Jones, 1981). If m limbs are used then the hypothsis of a common true mean direction is rejected if

$$\frac{(N - m)}{(m - 1)} \quad \frac{\sum R_i - R^2 / \sum R_i}{2\ (N - \sum R_i)} = f \ > \ F\ [2(m - 1),\ 2(N - m)]$$

where R is the length of the resultant vector of all site-mean directions, N is the number of sites and R_i are the length of the resultant vector of site-mean directions for each limb. F [a,b] is the F-distribution with a and b degrees of freedom.

In this case, there are five limbs:

-Miller's Ridge Horiz.: 173, -69 $N_1 = 5$

	Bedd. : 173, -69	R_1 = 4.790
-Five Finger	H: 188, -72	N_2 = 2
	B: 171, -72	R_2 = 1.943
-Glenlyon	H: 121, -71	N_3 = 1
	B: 176, -68	R_3 = 1
-Pilot Mtn	H: 117, -85	N_4 = 5
	B: 147, -76	R_4 = 4.865
-Table Mtn	H: 195, -63	N_5 = 5
	B: 170, -70	R_5 = 4.952

Globally,

H : 178, -73 R_H= 17.385 B : 167, -71 R_B= 17.680

$$\sum R_i = 17.73$$

f_H = 4.111 f_B = 0.601

F[8, 26] = 2.32 (at 95% confidence)

Conclusion : they share a mean direction with respect to bedding at more than 95% confidence.

The pole obtained by averaging paleopoles calculated for each site is 109.4°E, 82.1°N, A_{95} = 7.8° and K = 21.

Reversals and paleosecular variation

The mean direction of the normal (2 sites) and reversed (16 sites) groups are nearly antipodal (172° apart). Because the geomagnetic field was of normal polarity about 50% of the time from 73 to 68 Ma (Harland *et al.*, 1982), more than two normal polarity sites would be expected if the sampling had spanned several polarity intervals. There were, however, longer periods of single

polarity (up to 1.5 Ma) during this time interval. The fact that a polarity reversal is observed is an indication that the magnetization of the Carmacks group probably spans sufficient time to average the effects of secular variation. This conclusion may be further tested by examining the angular dispersion (Sd) of the site-mean paleopoles. The mean value of Sd is 17.7° and the limits for this value, at 95% confidence, are 14.5° and 22.9° (Cox, 1969). These limits show good concordance with the paleosecular variation model for the period 110-45 Ma (McFadden and McElhinny, 1984; Fig. 16). This agreement, combined with the presence of a polarity reversal, indicates that the data have adequately averaged the paleosecular variation. Therefore, the mean paleopole obtained for the Carmacks group is probably representative of a geocentric axial dipole (GAD) field.

Timing of acquisition of magnetization

There are two rock-units younger than the Carmacks group in the Whitehorse Trough: some Eocene volcanic centres scattered about Sloko, Bennett Lake and Skukum, and the Pleistocene Selkirk Lavas, but neither of these units can be used to establish a younger limit on the timing of deformation. However, Templeman-Kluit (1976) suggests that gentle tilting of the Carmacks group occurred during or shortly after eruption. Furthermore, there is no evidence in the geochronology (Grond *et al.*,

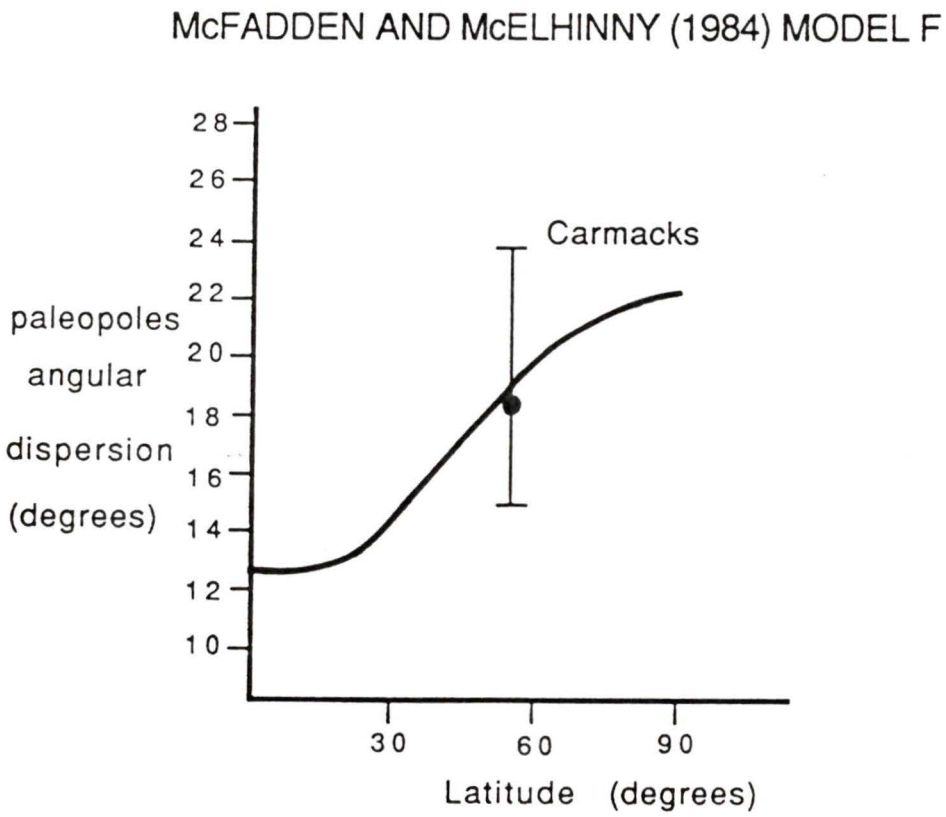

Figure 16. Comparison of angular dispersion of the paloepoles from the Carmacks group with the paleosecular variation model of McFadden and McElhinny (1984).

1984; Lowey *et al.*, 1986) for a reheating event caused by later volcanism, plutonism or deep burial. In summary, the available evidence indicates that the magnetization was acquired shortly after eruption in latest Cretaceous time, about 70 Ma. Because the maximum coherence of site-mean directions result from complete rather than partial unfolding of the beds, it is unlikely that the magnetization conicided with deformation.

North American cratonic reference pole

To establish the North American cratonic reference pole for latest Cretaceous time, several reliably dated paleopoles have been averaged using a 15 Ma window centred at 70 Ma. Irving and Irving's (1982) paleopole list was updated as follows. The Late Cretaceous Elkhorn Volcanics and the Jefferson Valley sequence in Montana (Hanna, 1967) have been omitted because there is an error in the calculations for tilt correction. The Niobara Formation of Kansas-Colorado-Wyoming has also been omitted because this rock-unit is now considered early Late Cretaceous in age (Gordon *et al*, 1984), i.e. too old for this compilation. I added the 72.7 +/- 4.2 Ma Roskruge Volcanics of Arizona (Vugteveen *et al.*, 1981), despite the fact that only 9 sites are reported, since both polarities are observed indicating that the secular

Table 7

Cratonic poles for latest Cretaceous and Paleocene

	Age (Ma)	Rock Unit	Pole (°E,°N)	A°_{95}
1.	64.3+/-2.1	Alkalic Intrusions, Montana (N=35)	181.4,81.8	5.4
2.	63.3+/-1.8	Gringo Gulch Volcanics, Arizona	201.0,77.0	1.5
3.	72.7+/-4.2	Roskruge Volcanics, Arizona	176.0,73.6	7.7

(1) Diehl *et al.* (1983); (2) and (3) Vugteveen *et al.* (1981).

variation has been adequately averaged. I also added 35 Paleocene sites from the Early Tertiary (64.3 +/- 2.1 Ma) Alkalic Intrusions of Montana (Diehl *et al.*, 1983). Together with the Paleocene (63.3 +/- 1.8 Ma) Gringo Gulch Volcanics of Arizona (Vugteveen *et al.*, 1981), these selected paleopoles give a mean cratonic North American reference pole at 185.8°E, 77.7°N, K = 255 (Table 7).

Displacement and rotation of the Carmacks group

A comparison of the paleopoles obtained for the Carmacks group and the North American craton suggests a 13.4° +/- 8.5° northward displacement and a 10.2° +/- 20.7° clockwise rotation of the Carmacks group relative to the craton, using the methods described in the introduction. The latter is not significant at 95% confidence. Hence the Whitehorse Trough has undergone some 1500 km +/- 950 km of northward displacement relative to the North American craton since 70 Ma (Fig. 17).

5.*Discussion*

The Carmacks group overlies portions of the Intermontane Superterrane, which is composed of Stikinia, Cache Creek, Quesnellia and Slide Mountain terranes (Wheeler and McFeely, 1987). These elements of Baja British Columbia were amalgamated by latest Jurassic-earliest Cretaceous time, prior to its accretion to the ancient margin of western North America (Monger *et al.*,

1982). The amount and timing of post-amalgamation northward translation of Baja British Columbia is a fundamental problem in the evolution of the Cordillera.

Comparison with motions on faults

The Whitehorse Trough is separated from the Selwyn Basin of the North American Craton to the east by the Tintina- Northern Rocky Mountain Trench (TRNMT) fault (Fig. 8). The post 70 Ma northward translation obtained above implies significant dextral motion on the TRNMT fault since latest Cretaceous time. A face-value interpretation of the displacement estimate (1500 +/- 950 km) exceeds the minimum value of dextral offset on the Tintina Trench fault alone (450 km) as proposed by Roddick (1967). It is consistent with the larger value of dextral offset of more than 900 km estimated by Gabrielse (1985) for the TRNMT fault and associated lineaments in northern British Columbia. Timing of the motion on the faults described by Gabrielse ranges from mid-Late Cretaceous to perhaps Eocene, a time range also consistent with the time interval of displacement indicated by the Carmacks group's data.

Comparison of displacements for plutonic and volcanic rock-units

A second useful application of the paleomagnetic data for the Carmacks group is to compare estimates of the northward displacement obtained from bedded volcanic

strata in the Whitehorse Trough with those obtained from intrusive rocks in the Coast Plutonic Complex (CPC) of southwest British Columbia and northwest Washington. This is important because a number of paleomagnetic studies of mid-Cretaceous intrusions in the CPC suggest large scale ($\approx 25^{\circ}$) northward displacement (see Irving *et al.*, 1985). The consistency of anomalously shallow paleolatitudes observed in several intrusions argues for displacements from the south. Since these units are intrusions in which bedding cannot be directly measured, the aberrancy in direction could have been ascribed incorrectly to translation rather than geological tilt. However, the northward displacement of 13.4° +/- 8.5° for the Carmacks group (whose attitudes are well known) makes the displacements observed for the CPC intrusions more plausible. Note that the Carmacks group is about 20 to 30 Ma younger than the intrusions, so that the latter may have undergone some northward translation prior to the eruption of the Carmacks group. This argues against a tilting explanation of the aberrancy in direction for the CPC intrusions, although more paleomagnetic studies of Cordilleran volcanic rock-units, specially early or mid- Cretaceous in age, will be required to rule it out completely.

Comparison with plate tectonic models

The observed northward displacement could have been

caused if the Carmacks group and its basement were attached to the Kula plate (Beck *et al.*, 1981b; Debiche *et al.*, 1987). But are the hypothesized motions of the Kula plate consistent with the paleomagnetic evidence? Using the Euler poles and rotation angles describing the motion of the Kula plate relative to North America (Engebretson *et al.*, 1985; Table 8), possible trajectories (Kula trajectory models) were calculated for the Carmacks group, assuming docking times of 60, 55 and 50 Ma (Fig. 17). These trajectories assume perfect coupling between the Carmacks group and its basement and the Kula plate. The modelled latitude of formation of the Carmacks group is in good agreement with the paleomagnetic estimate if docking times of 60 or 55 Ma are assumed. If a later docking time of 50 Ma is postulated, the modelled paleolatitude is shallower (Fig. 17). Furthermore, the trajectory models suggest significant clockwise rotations, rotations which could be accommodated by the large errors in the paleomagnetic data. The Kula trajectories also imply longitudinal motion of the Intermontane Superterrane, which means that a large area of crust (approximately the stippled triangle of Fig. 17 with OP at its centre) has been destroyed between the Intermontane Superterrane and cratonic North America. This is highly improbable, since most of the faults on the North American craton that

Table 8

Euler poles and rotation angles describing the motion of the Kula plate relatve to North America

Age (Ma)	Euler pole (°N, °E)	Rot. angle
43	-------	----
48	-7, 303	9.4
56	-7, 298	15.4
61	-6, 278	5.6
66	-3, 285	6.6
70	5, 288	5.8

Euler poles in a fixed hotspot frame. The rotations given are those that will restore the Kula plate to its positions at times shown in the left-hand column. From Engebretson *et al.* (1985).

PALEOLATITUDE AND KULA PLATE TRAJECTORIES

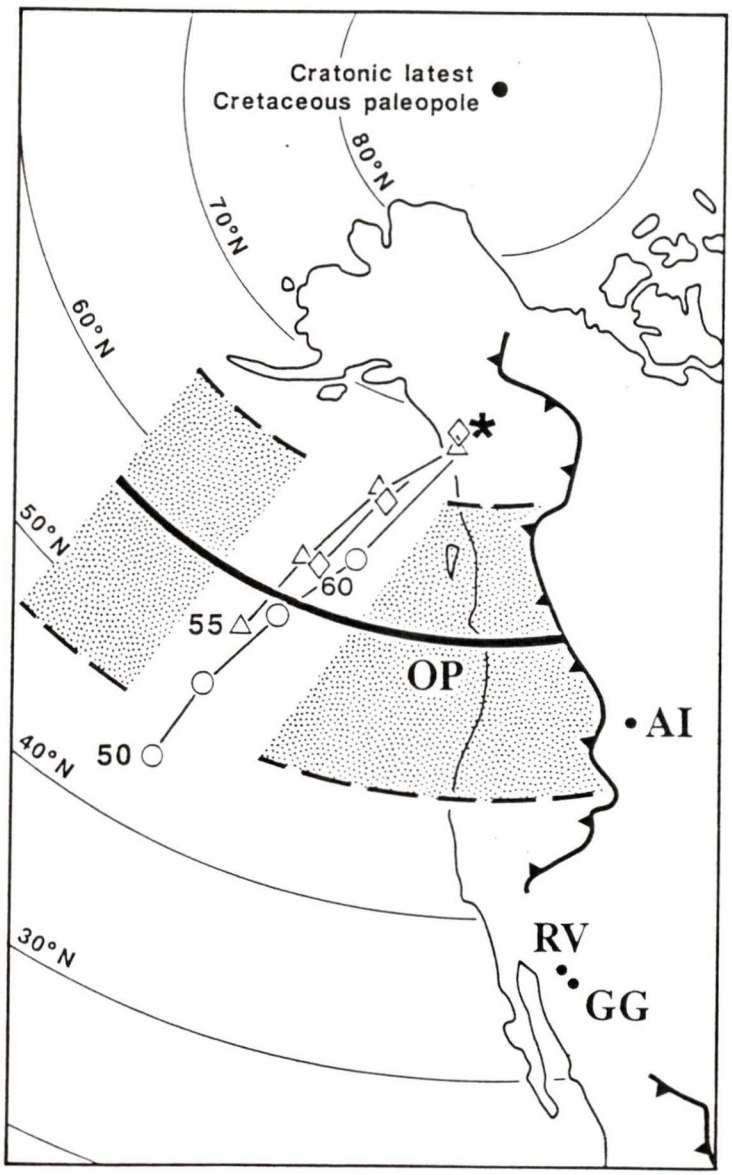

Figure 17. Observed paleolatitude (OP) and error zone of the Carmacks group. Lines connecting open symbols represent trajectories for the Carmacks group and their related docking times, in Ma. Cratonic poles : GG, Gringo Gulch volcanics; RV, Roskruge Volcanics; AI, Alkalic Intrusions.

were active between Late Cretaceous and Tertiary time are strike-slip faults, i.e. indicators of transcurrent motion (Gabrielse *et.al*, in press). Hence, the coupling between the Carmacks group and the Kula plate was probably not perfect, specifically for the longitudinal component of motion.

A model developed by Umhoefer (1987) accommodates this imperfect coupling. He assumes that the motion of the Kula plate relative to North America was almost pure transform (Baja B.C. coupled at $\approx$100% with Kula plate) between 85 and 66 Ma, along the north-trending margin of the North American plate. Prior to 66 Ma, the Kula plate was subducting farther north. A plate reorganization at 66 Ma shifted the locus of Kula plate subduction to more southerly latitudes. This shift resulted in a dextral oblique-convergent (i.e. transpressionnal margin between Kula and North America plates west of Baja British Columbia (Fig. 18)). From then on, northward motion of the Carmacks group (CK) occurred along inboard dextral faults, resulting in a cumulative displacement of about 1000 km. Umhoefer's scenario, summarized in Fig. 18, is consistent with Gabrielse's estimate of dextral offset on the TRNMT fault system (1985), and is in excellent agreement with the displacement observed paleomagnetically for the Carmacks group in the

UMHOEFER'S (1987) MODEL FOR "BAJA BRITISH COLUMBIA"

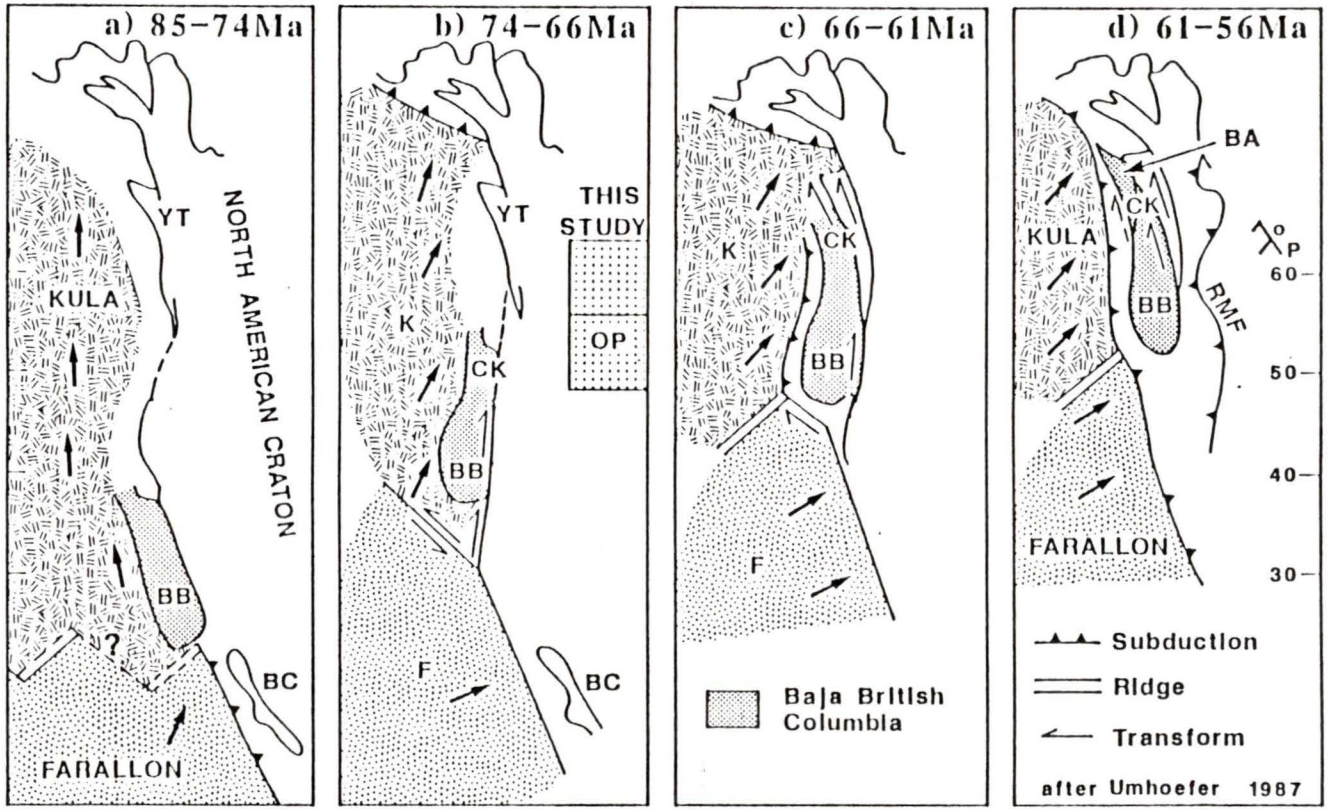

Figure 18. Comparison of the Carmacks group (CK) paleolatitude with this model. BA, Baja Alaska; BB, Baja British Columbia; BC, Baja California; RMF, Rocky Mountain Fault; YT, Yukon-Tanana terrane.

Whitehorse Trough as shown in Fig. 18b.

Docking time

There is no evidence from Baja British Columbia, in Yukon and British Columbia, constraining the time of displacement of the Carmacks group. However, paleomagnetic data are available from the Cantwell Formation in the central Alaska Range (Hillhouse and Grommé, 1982). This formation is spatially related to the Carmacks group (between Tintina and Denali faults), although it is younger (Tertiary). Hillhouse and Grommé (1982) report 9° +/- 8° of southward displacement of the Cantwell Formation relative to North America, assuming an age of 56.6 +/- 2.8 Ma (recalculated using the revised decay constants of Steiger and Jäger, 1977). This displacement estimate being barely significant at 95% confidence, the paleolatitude of the Cantwell Formation can be said to be essentially concordant with that expected for the craton in Late Paleocene time. This implies a final docking time of about 59 to 54 Ma for the Whitehorse Trough, limits consistent with the paleomagnetic data (Fig. 17).

CHAPTER III EOCENE "CORYELL" SYENITES AND ASSOCIATED METAMORPHIC ROCKS

1. *Introduction*

This chapter is concerned with aberrant magnetizations that can, I shall argue, be explained better by geological tilting rather than by translation or rotation. This work is really a test of the idea that paleomagnetism can be used to determine tilt in deep crustal rocks in areas undergoing strong uplift and extension (Bardoux and Irving, in preparation). This is a matter of relevance to LITHOPROBE, which is scheduled to pass in the areas studied here.

The western Cordillera in Canada has been formed by the accretion of allotochtonous terranes to the ancient margin of North America (as discussed in Chapter II) and by the deformation of this margin during the accretionary process. Although there is much discussion about the nature and timing of these processes, there is a general agreement that the terranes had reached their present positions by the time the major deformation in the Fold and Thrust Belt had ceased, by Eocene time. Paleomagnetic data from the Early to Mid-Eocene volcanics of the Kelowna Outlier (Bardoux and Irving, in preparation) confirm this assumption.

The Omineca Belt is the eastern metamorphic core zone of the Cordilleran orogen. Extensive Eocene uplift and

extension contributed significantly to the present crustal structure of the southern Omineca Belt in British Columbia and Washington (Parrish *et al.*, 1988). Evidence for that extension include Eocene normal faults juxtaposing low grade metamorphic rocks with granitic gneiss and metamorphic rocks which were at mid-crustal levels in the Paleocene (Fig. 19).

Such extension has caused uplift and denudation of the middle crust comprising metamorphic rocks of amphibolite grade (with mineralogies stable around 600°C) later intruded by syenitic plutons and dikes. As these rocks cooled they became magnetized as they got closer to the surface. During uplift the crust has fractured, and this fracturing took the form of large low-angle normal extensional faults, and subordinate steep brittle normal faults roughly parallel to the principal extensional fault (Wernicke, 1985). This fracturing has caused tilting approximately equal to the dip of the large normal fault, but in a sense opposite to that of the fault (Fig. 5).

In this second example, I present paleomagnetic data from two plutons, and from a sequence of dikes and metamorphic rocks. The tilt correction needed to bring the observed direction to the expected direction will yield the amount of Eocene tilting of the crust. This is an important observation because the mid-crustal

MAP OF THE SOUTHERN OMINECA BELT AND ITS NORMAL EXTENSIONAL FAULTS

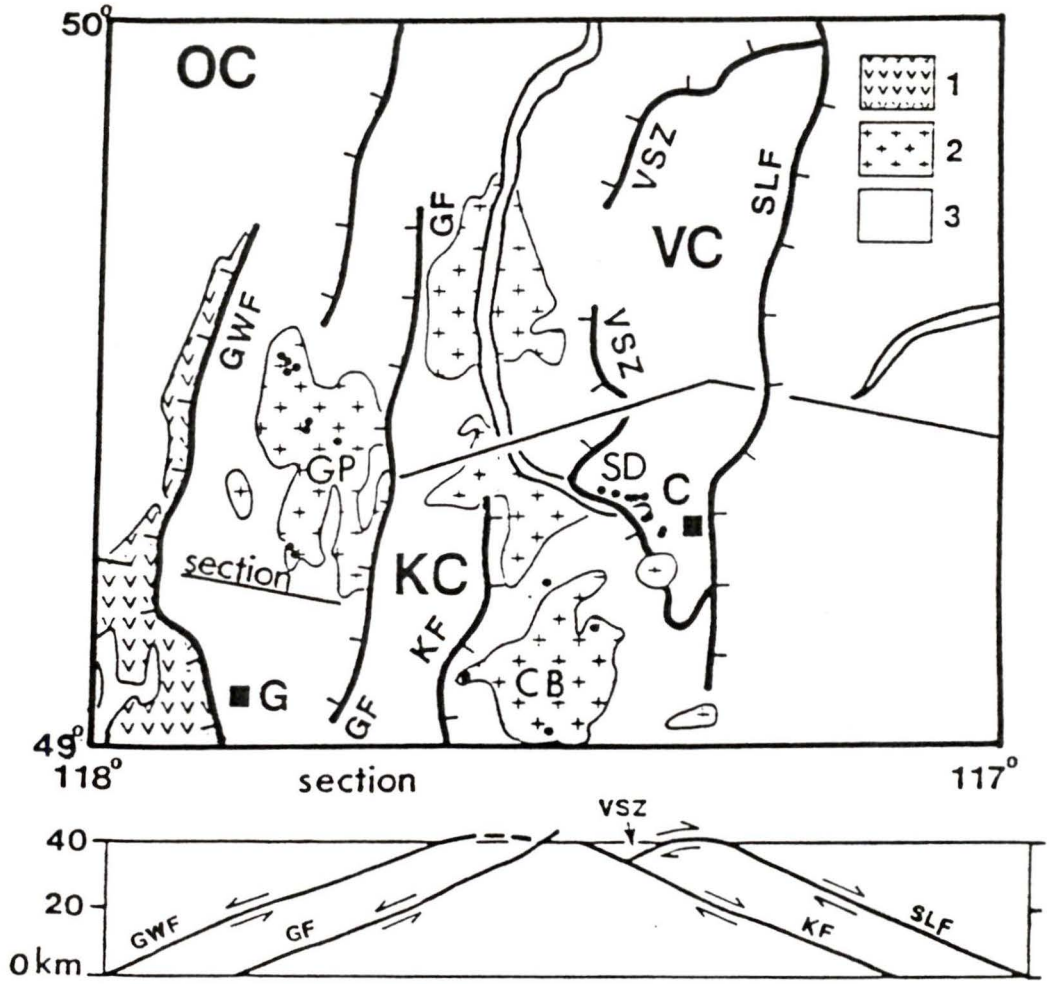

Figure 19. Tectonic map of the southern Omineca belt. 1, Middle Eocene volcanic and sedimentary rocks; 2, Middle Eocene syenite, granite; 3, Pre-Eocene rocks. Normal faults (peg on upper plate): GWF, Greenwood fault; GF, Granby River fault; KF, Kettle River fault; VSZ, Valkyr Shear Zone; SLF, Slocan Lake fault. Metamorphic complexes: OC, Okanagan; KC, Kettle-Grand Forks; VC, Valhalla. Sampling areas: GP, Granby Pluton; CB, Coryell Batholith; SD, Syringa Dikes and associated metamorphic rocks. Towns: G, Greenwood; C, Castlegar. Black dots denote sampling sites. From Parrish *et al.* (1988).

rocks themselves do not contain any evidence of the paleohorizontal and hence tilt cannot be determined by standard geological procedures.

2. *Geology and sampling*

A map of the sampling area is shown in figure 19. The main tectonic elements are the Granby River fault, the Kettle River fault, the Valkyr Shear Zone and the Slocan Lake fault. These faults contributed to the extension of the southern Omineca Belt in Eocene time.

Granby River fault

The Granby River fault was first mapped by Little (1957). It bounds the west margin of the Kettle-Grand Forks metamorphic complex. It dips to the west and cuts $\approx$ 52 Ma "Coryell" syenites and the Middle Eocene Marron Formation.

Kettle River fault

The Kettle River fault separates the high-grade Kettle-Grand Forks metamorphic complex from lower grade metamorphic, volcanic and plutonic rocks to the east. It is an easterly dipping brittle extensional fault (Rhodes and Cheney, 1981). It is cut by "Coryell" syenites in the north, but it cuts "Coryell" syenites in the South. Its movement therefore implies both Early and Middle Eocene displacement (Parrish *et al.*, 1988).

Valkyr Shear Zone

The Valkyr Shear Zone forms the roof of the Valhalla Complex. Its displacement followed closely the emplacement of the ≈56 Ma Ladybird Granite. It is also cut by ≈52 Ma "Coryell" syenites about 10 km west of Castlegar. Hence it is the oldest of these large extensional shear zones.

Slocan Lake fault

The Slocan Lake fault bounds the Valhalla Complex to the east (Parrish, 1984). It dips to the east and cuts the Valkyr Shear Zone (Carr *et al.*, 1987).

Since the intrusion of the "Coryell" syenites is used as a time boundary for the movements on these faults, the determination of its post-intrusion tilt can provide information on the later stages of the extensional process in the area. Two plutons of "Coryell" syenites have been sampled : the Coryell Batholith itself and a pluton located north of Grand Forks which is tentatively named "Granby" Pluton. The Syringa Dikes, which are interpreted as being contemporaneous with "Coryell" syenites (Parrish, 1988) have also been extensively sampled (Table 10).

"Granby" Pluton

It is located about 15 km north of Grand Forks, west of the Granby River fault. Most of the rocks collected

are fine-grained diorites, with sometimes higher proportions of quartz and mica. A sequence between sites 19 to 16 spans about 500 m vertically. Most of the other sites were sampled by the Granby river. Site 14 is from a Coryell dike, which cut the Granby Pluton shortly after intrusion (Jim Fyles, personal communication).

Coryell Batholith

Located west of Rossland, east of the Kettle River fault, we sampled mainly coarse-grained micaceous diorites. Three areas were sampled: Nancy Greene Park, along former Highway 3 and by Christina Lake (where fine-grained diorites were collected). A large proportion of the sampled material showed some degree of weathering, it is therefore not surprising that only four sites yielded satisfactory paleomagnetic data. K/Ar radiometric ages are available (Armstrong, unpublished data file), they range from 49.1 to 49.9 Ma (Table 9).

Syringa dikes and associated metamorphic rocks

These are located west of Castlegar, along the Lower Arrow Lake, west of the Slocan Lake fault, but east of the Valkyr Shear Zone. The dikes are subvertical and are disseminated through the Castlegar Gneiss Complex. Most of the material sampled consists of fine-grained metamorphosed mica diorite. Also, a few

Table 9

Collecting sites, "Coryell" syenites

Site no.	Rock type	UTM coordinates (grid zone 11U)
CORYELL BATHOLITH		
TCS-01	horn. diorite	4229E-54528N
TCS-03	quartz diorite	4359E-54490N
TCS-06	quartz diorite	4253E-54305N
TCS-11	quartz diorite	4110E-54402N
TCS-12	mica diorite	4111E-54391N
GRANBY PLUTON		
TCS-13	quartz diorite	3906E-54504N
TCS-14	plagio. diorite	3916E-54495N
TCS-16	quartz diorite	3859E-54812N
TCS-17	diorite	3867E-54805N
TCS-18	mica diorite	3869E-54800N
TCS-19	mica diorite	3884E-54795N
TCS-20	quartz diorite	3900E-54748N
TCS-21	diorite	3899E-54749N
TCS-22	diorite	3954E-54725N

Table 9 (continued)

Site no.	Rock type	UTM coordinates (grid zone 11U)
SYRINGA DIKES AND ASSOCIATED METAMORPHIC ROCKS		
TSG-52	mica diorite	4284E-54719N
TSG-54	mica diorite	4300E-54699N
TSG-56	mica diorite	4342E-54675N
TSG-57	diorite	4363E-54662N
TSG-58	mica diorite	4494E-54577N
TSG-59	mica diorite	4493E-54577N
TSP-01+	diorite	4375E-54658N
TSP-02+	diorite	4375E-54659N
TSP-05+	diorite	4420E-54650N
TSP-06+	dioritic gneiss	4422E-54650N
TSP-07+	diorite	4425E-54648N

NOTES: + data from Bardoux and Irving (In preparation)

Table 10

Radiometric dates for "Coryell" syenites

Area	UTM coordinates (grid zone 11U)	Method	Age (Ma)
Syringa dikes	4376E-54658N	U/Pb zircon	51.5 +/- 0.5
Coryell	4402E-54400N	K/Ar biotite	49.8 +/- 1.4
Batholith	4420E-54364N	" "	49.9 +/- 1.5
	4374E-54403N	" "	49.1 +/- 1.4

Date for Syringa from Parrish *et al* (1988) and for Coryell from Armstrong (unpublished data file, reported in Fyles (1984).

SYRINGA DIKE

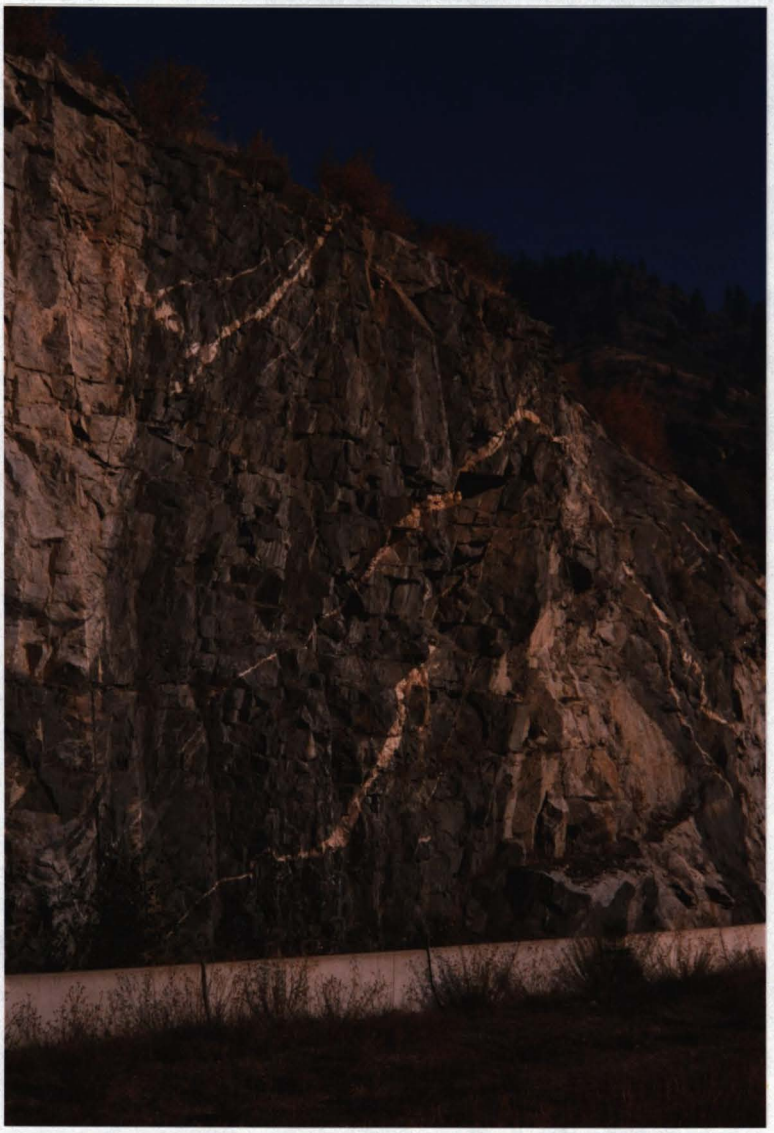

Figure 20. Syringa dike intruding the Castlegar Gneiss, on the north shore of Arrow Lake.

unmetamorphosed dikes have been collected, but only one (57) gave consistent paleomagnetic data. One U/Pb radiometric date is available from a "Coryell" syenite to which the dikes are associated: 51.5 +/- 0.5 Ma (Table 9).

3.*Magnetizations*

The methods used and the classification criteria are the same as for the previous study (Table 11). The optimum cleaning field was 20 mT for most sites. A-type magnetization, demagnetized by AF, is shown in figure 21. The low coercivity (10 mT) overprint is approximately parallel to the PEF, therefore probably a VRM. The principal magnetization is well defined by a linear decay to the origin of the orthogonal plots and by an end-point reached at cleaning fields of 20 mT and higher.

AF demagnetization of a B-type magnetization is shown in figure 22. Although the orthogonal plots show linear decay to the origin, the magnetization vector wobbles about a crude end-point. The principal magnetization has been obtained using a least-squares best-fit analysis and is shown by a star. The other example of B-type magnetization (Fig. 23) shows linear decay on the orthogonal plots, but not to the origin, indicating that a high-coercivity magnetization is present. As in the

Table 11

Quality of paleomagnetic data, "Coryell" syenites

Site	A, B, C	Site	A, B, C
GRANBY PLUTON		CORYELL BATHOLITH	
TCS-13	2,10, 3	TCS-01	14, 0, 0
TCS-14	10, 2, 0	TCS-03	1, 4, 5
TCS-16	5, 6, 1	TCS-06	0, 6, 1
TCS-17	6,10, 0	TCS-11	9, 0, 0
TCS-18	0, 7, 0	TCS-12	13, 0, 0
TCS-19	2, 6, 0		
TCS-20	10, 0, 0		
TCS-21	9, 1, 0		
TCS-22	3, 6, 0		
SYRINGA DIKES AND ASSOCIATED METAMORPHIC ROCKS			
TSG-52	0,10, 0		
TSG-54	10, 0, 0		
TSG-56	10, 0, 0		
TSG-57	8, 2, 0		
TSG-58	10, 0, 0		
TSG-59	13, 0, 1		

Data from Bardoux and Irving not included.

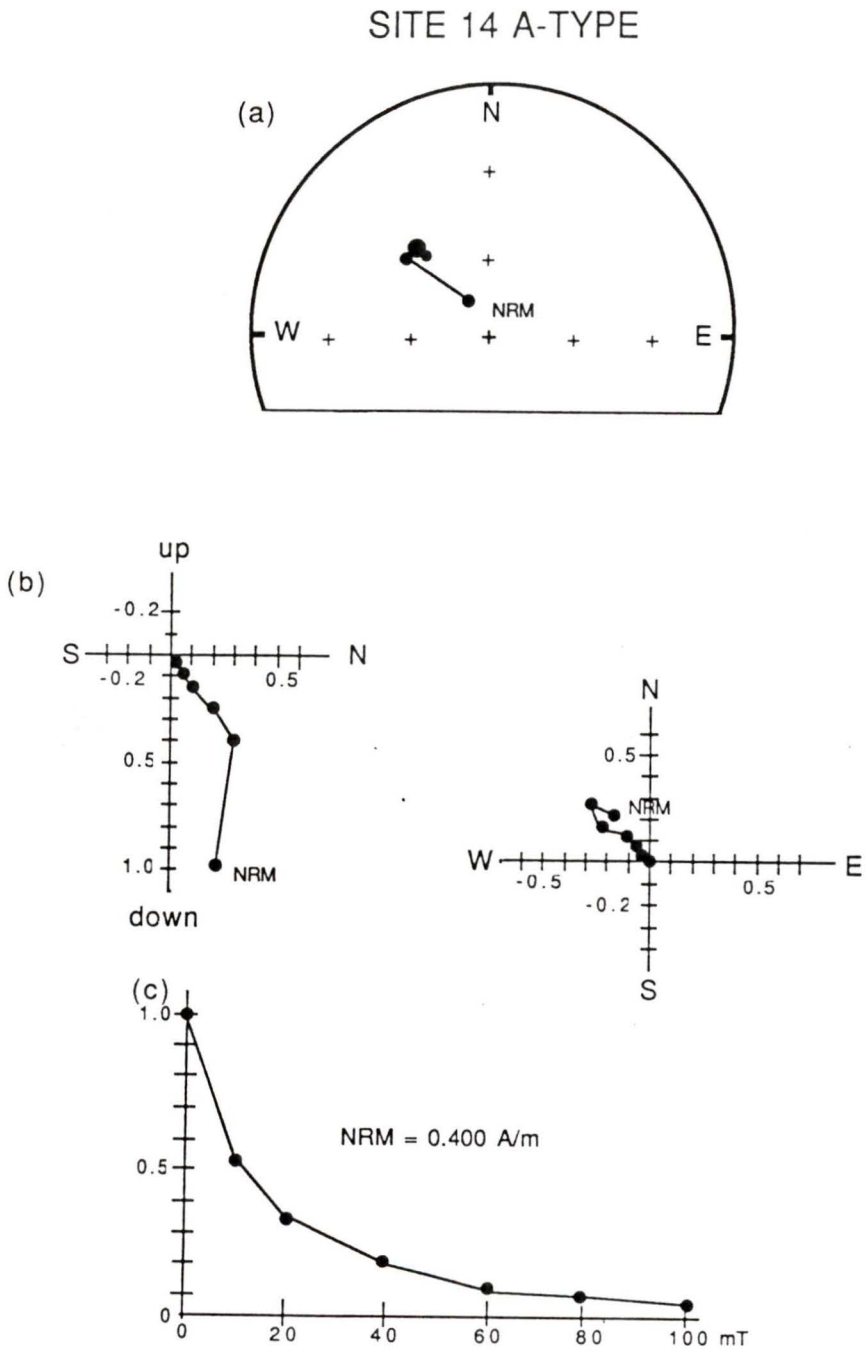

Figure 21. AF demagnetization of A-type magnetization. A low-coercivity magnetization (probably VRM) overprinted the principal magnetization. Same conventions than in figure 9.

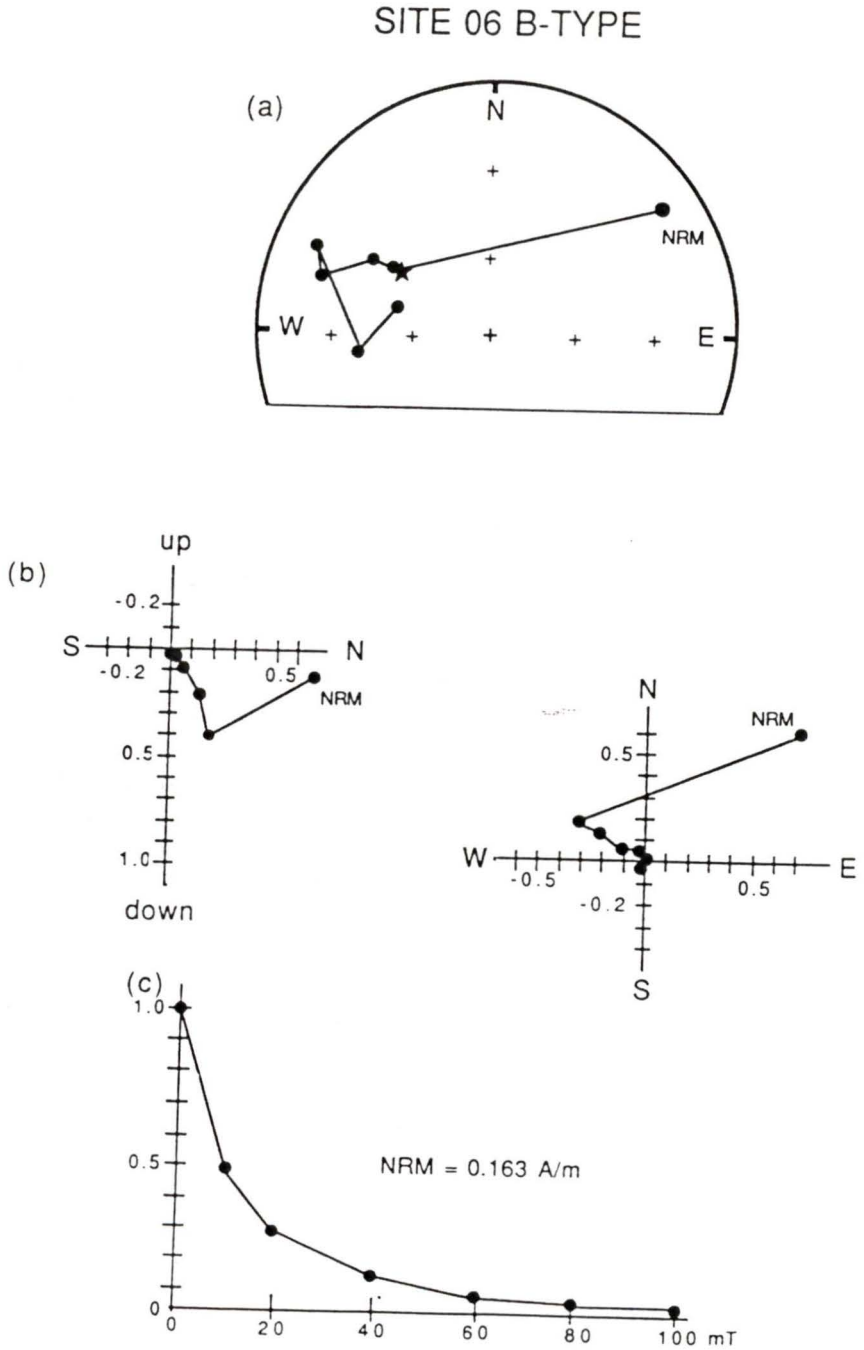

Figure 22. AF demagnetization of B-type magnetization. No end-point, but linear decay to the origin.

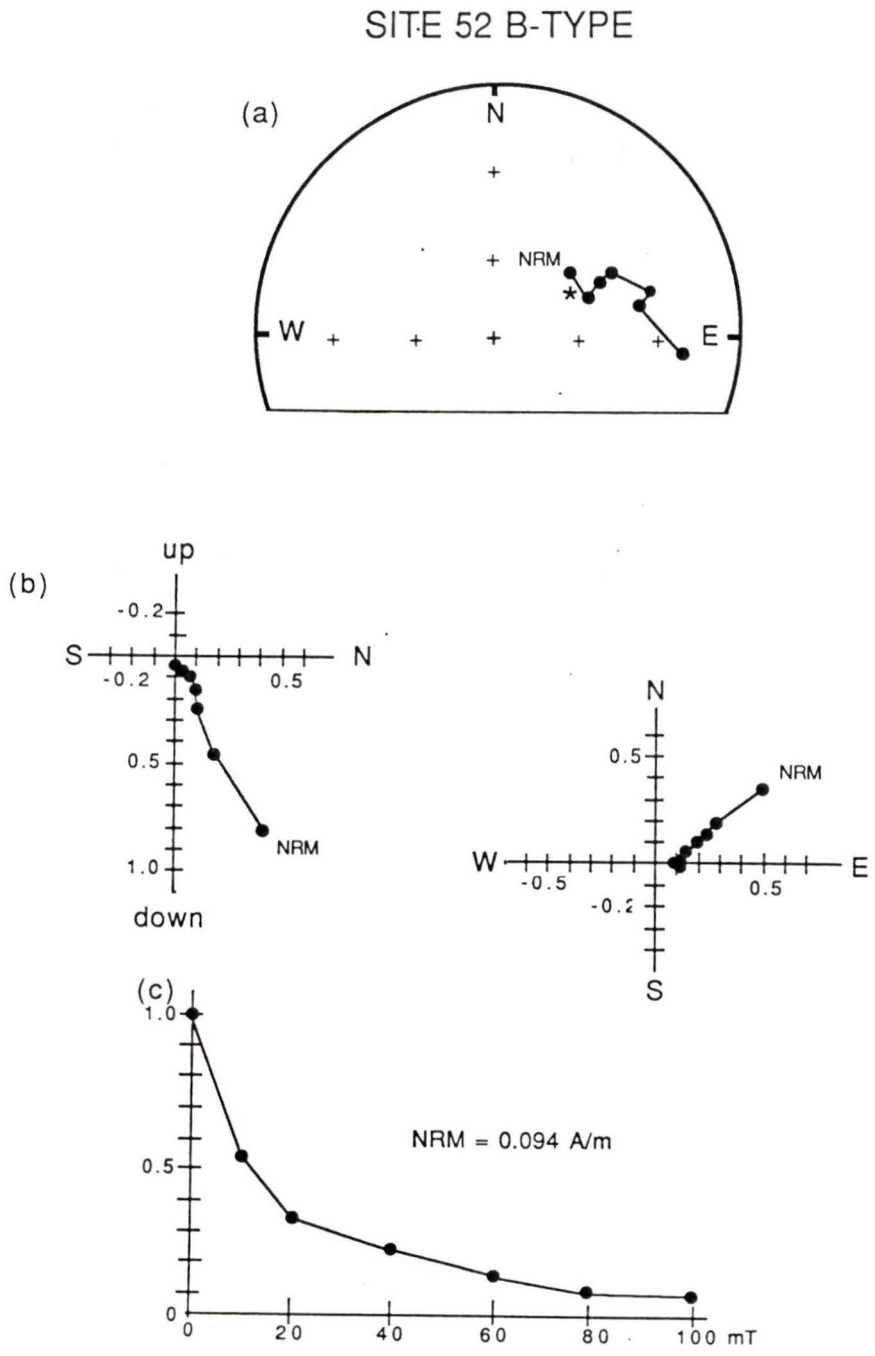

Figure 23. AF demagnetization of B-type magnetization. In this case, the lines do not decay to the origin indicating the presence of a small, high-coercivity magnetization.

Table 12

Paleomagnetic data, "Coryell" syenites

Site	n, s, s'	D°, I°	k	α_{95}	Pole (λ, φ)
CORYELL BATHOLITH					
TCS-01	7,14,12	285, 25	59	6	20, 149
TCS-03	5,10, 5	331, 49	24	16	61, 121
TCS-06*	4, 6, 6	306, 58	98	7	51, 158
TCS-11	6,12,10	310, 40	124	4	43, 137
TCS-12	7,13,13	302, 31	83	5	33, 138
GRANBY PLUTON					
TCS-13	8,15,12	318, 66	64	6	62, 166
TCS-14	6,12,12	303, 43	49	6	40, 145
TCS-16	6,12,11	327, 58	50	7	64, 139
TCS-17	8,16,16	304, 27	79	4	33, 134
TCS-18	5, 7, 7	308, 16	119	6	30, 126
TCS-19	6,12, 8	340, 41	31	10	59, 99
TCS-20	5,10,10	304, 44	179	4	41, 144
TCS-21	5,10,10	308, 40	139	4	42, 137
TCS-22	5, 9, 9	283, 20	59	7	16, 149
SYRINGA DIKES AND ASSOCIATED METAMORPHIC ROCKS					
TSG-52	5,10,10	57, 56	39	8	47, 328
TSG-54	5,10,10	55, 51	104	5	45, 334

Table 12 (continued)

Site	n, s, s'	D°, I°	k	α_{95}	Pole (λ, φ)
TSG-56	5,10,10	245,-54	95	5	41, 324
TSG-57	5,10,10	235,-40	201	3	40, 344
TSG-58	5,10,10	50, 42	368	3	44, 347
TSG-59	9,14,13	38, 42	79	5	51, 359
TSP-01	5,10,10	227,-34	74	6	42, 354
TSP-02	5, 9, 9	69, 52	25	10	38, 323
TSP-05	6,12,12	68, 51	14	12	37, 324
TSP-06	5,10, 9	65, 37	77	6	32, 337
TSP-07	5,10,10	52, 54	20	11	50, 333

n, number of cores collected; s, number of specimens; s',number of specimens used in calculating site-mean directions; D°, I°,declination and inclination of the mean direction; k, estimate of Fisher (1953) precision parameter; α°_{95}, half-angle of cone of 95% confidence; λ°, φ°, latitude (°N) and longitude (°E) of paleopole; *, site showing both polarities.

previous example, the least-squares best-fit principal magnetization is shown by a star.

C-type magnetizations were also observed. They were usually present in coarse-grained and more felsic rocks collected in the Coryell Batholith and in the unmetamorphosed Syringa Dikes. These rocks have very low coercivity and essentially random directions. They provide no record of the paleofield and hence have been rejected from the analysis.

4. *Analysis and Interpretation*

Reference field for Eocene

To establish the reference field for Eocene time for North America, the paleopole list of Irving and Irving (1982) has been updated. I added the data from the Kelowna Outlier (Bardoux and Irving, in preparation), since they show that it was part of stable North America in Eocene time. This gives a North American pole for the interval 54-44 Ma at 177.9°E, 84.9°N, A_{95} = 4.4° (Table 13), or an expected paleofield of D = 353°, I = 69°, α_{95} = 3° (Table 14).

The site-mean directions (Table 12), their means and their standard errors (α_{63}) for each of the plutons studied (Table 14) are plotted in figures 24 to 26.

Table 13

Cratonic poles for the interval 54-44 Ma

	Age (Ma)	Rock-Unit	Pole(°N,°E)	A°_{95}
1.	44-52	Kelowna Outlier, BC.	85.0,181.0	4.4
2.	47	Monterey Intrusives, Virginia	86.7,309.3	12.0
3.	48	Absaroka Supergroup Volcanics, Wyoming	83.5,177.4	10.1
4.	49-53	Highwood Mountain Volcanics, Montana	81.2,167.3	7.2
5.	50-54	Bear Paw Mountain Volcanics, Montana	82.0,170.2	3.5
MEAN POLE		(K = 307)	84.9,177.9	4.4

(1) Bardoux and Irving (in preparation); (2) Lovlie and Opdyke (1974); (3) Shive and Pruss (1977); (4) and (5) Diehl *et. al* (1983).

Table 14

Summary of data, "Coryell" syenites

	N	D°, I°	k	α_{63}	α_{95}	Pole (°N, °E)
CORYELL BATHOLITH						
Directions	5	305, 42	20	9	18	41, 142
Poles	5	-------	20	9	18	42, 142
GRANBY PLUTON						
Directions	9	309, 41	16	7	14	42, 137
Poles	9	-------	17	7	13	44, 138
SYRINGA DIKES AND ASSOCIATED METAMORPHIC ROCKS						
Directions	11	56, 47	63	3	6	56, 318
Poles	11	-------	58	3	6	56, 319
Expected paleopole	5	-------	307	2	4	85, 178
Expected direction	5	353, 69	568	2	3	-------

Granby Pluton

For the Granby Pluton, (Fig. 24), the site-mean directions are somewhat scattered, but there is no spatial relation of direction. The data indicate that the Granby Pluton has tilted on average 38° +/- 9° toward the east-south-east (102°). Some of the scatter could have been caused by variable tilting from site to site. The tilt observed paleomagnetically has presumably been caused by movement along the Granby River fault, which is known to be younger than the Granby Pluton. The Granby River fault is estimated to dip about 34° to the west at the surface (Parrish *et al.*, 1988) which is comparable to the tilt of 38° +/- 9° obtained from the Granby Pluton. Note that the direction of tilting is orthogonal to the strike of the fault, as expected. Such tilts have also been observed in bedded units west of the Greenwood fault (Jim Fyles, personnal communication).

Coryell Batholith

For the Coryell Batholith (Fig. 25), only five sites yielded consistent paleomagnetic data. The scatter is again fairly large. The data indicate a tilt of 40°+/-11° to the east (96°). Since the Coryell Batholith is located just east of the east-dipping Kettle River fault, one would expect not an easterly but a westerly

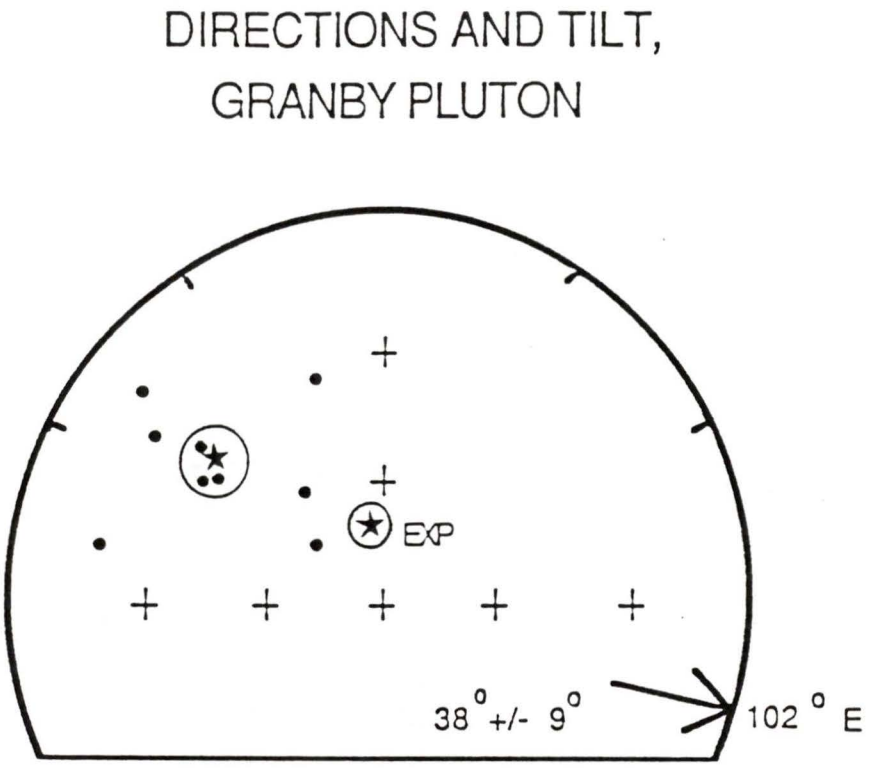

Figure 24. Site-mean directions for the Granby Pluton. They indicate a tilt of about 38° to the east.

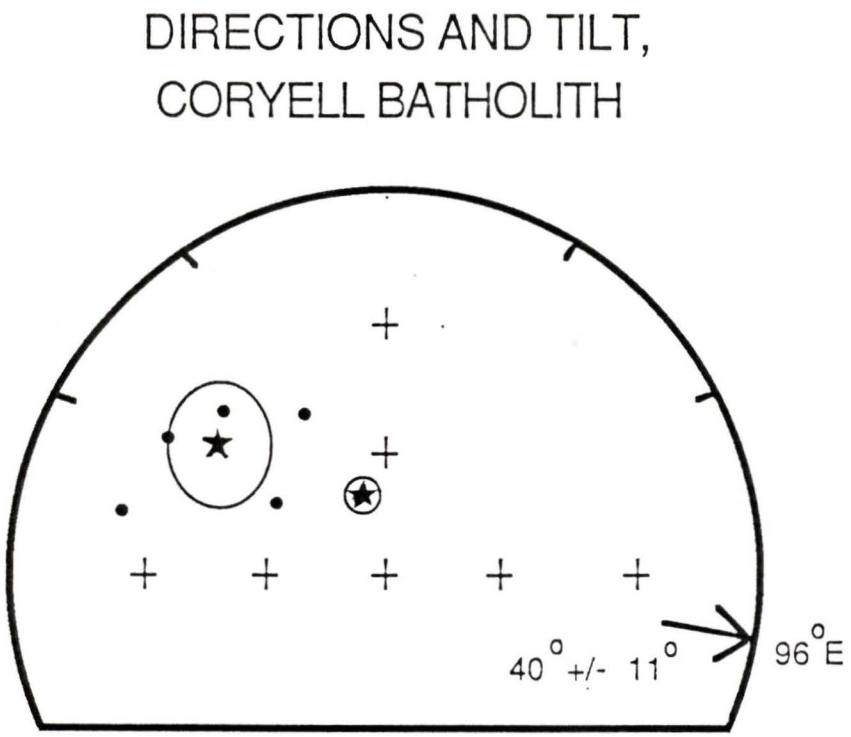

Figure 25. Site-mean directions for the Coryell Batholith. They indicate a tilt of about 40° to the east.

tilt. There are two situations which could have caused the easterly tilt inferred paleomagnetically. A two-stage process of tilting: to the west along the Kettle River fault (28°W), followed by a $\approx 68°$ tilt to the east, or a $\approx 40°$ tilt to the east only. The first hypothesis is very improbable, because it implies that the Coryell Batholith is younger than the Kettle River fault which is inconsistent with the geochronologic evidence. On the second hypothesis, the easterly tilt has to be caused by a west-dipping fault which would cut the Kettle River fault and reach the surface east of the Coryell Pluton. There is no record of such a fault in the literature, although the presence of west-dipping faults within the Coryell Batholith (O.K. and Snowdrop faults) has been reported by Fyles (1984). These however are not sufficient to explain the tilt since data from site TCS-03, which is located east of these faults, also indicate a westerly tilt.

Syringa Dikes and associated metamorphic rocks

Their data (Fig. 26) show excellent clustering. Both polarities are observed, in contrast to the other bodies where only normal magnetizations are present. The data indicate a westerly (266°) tilt of 39° +/- 5°. There is only one radiometric age available for them so that the sequential timing of their intrusion is not known. The

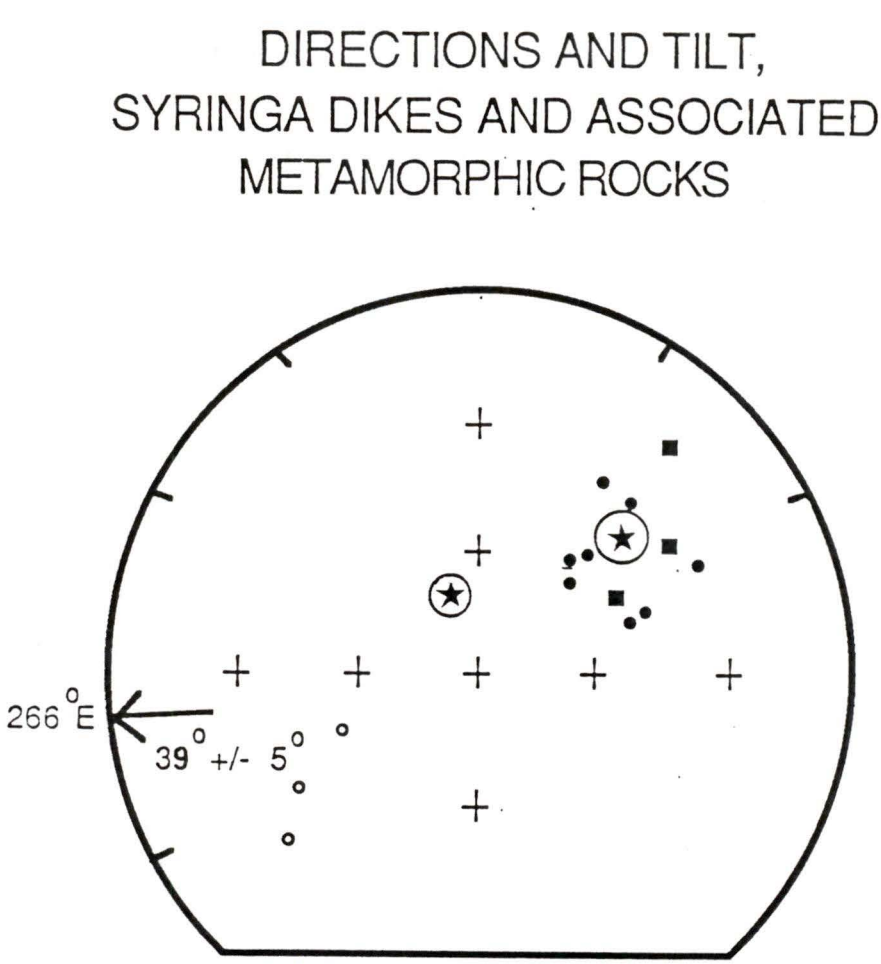

Figure 26. Site-mean directions for the Syringa Dikes and associated metamorphic rocks. They indicate a tilt of about 39° to the west.

only fault that can accommodate the tilt obtained paleomagnetically is the Kettle River fault. The fault dips about 28° to the east (Parrish *et al.*, 1988), which is somewhat shallower than the 39° +/- 5° obtained from the paleomagnetic data.

The additional 10° westward tilt that would be needed to satisfy the paleomagnetic data might have been caused by the latest part of the motion along the Valkyr Shear Zone. Such motion is possible since a field reversal is observed indicating that the Syringa Dikes' intrusion spanned an interval of time perhaps located between magnetic anomalies 23 and 22r. This is possible because most of the dikes show normal polarity (23 lasts longer than 22), and anomaly 22r, since it lasts longer than 23r, is more likely to have caused the observed reversed polarities. Obviously this time assignment is extremely speculative, but nevertheless it is a possible time correlation. Anomaly 23 begins at ≈52.5 Ma (Harland *et al.*, 1982). Since the Valkyr Shear Zone is presumed to be active from ≈56 to ≈52 Ma (Carr *et al.*, 1987; Parrish *et al.*, 1988), it is possible that some of the earlier Syringa Dikes intruded during the later part of that movement, therefore causing tilting slightly to the west before, in a second stage, tilting along the Kettle River fault. Again, this is very speculative, and more

geochronologic and paleomagnetic work will be needed to get a clearer picture of the timing of the different stages of the extensional process.

The westward tilt along east-dipping faults has also affected a large area to the east, since Bardoux and Irving (in preparation) report a westerly tilt of about 39° for a site of "Coryell" syenites located near Ymir, ≈ 30 km east of Castlegar. This also suggests that the intrusion of "Coryell" syenites happened in two or more phases, since this pluton would be approximately contemporaneous to the Syringa Dikes while the Coryell Batholith is younger than them.

5. *Conclusions*

Paleomagnetically determined tilts have been established and appear to be of a plausible magnitude. Data are still too few to establish a detailed picture, but it is possible that such paleomagnetically determined tilts can help in the interpretation of the tectonic history of this region. For example, using these data, one can speculate on the sequence of events accompanying the Eocene extension in the southern Omineca Belt:

1. 56 to 52 Ma. Motion on the Valkyr Shear Zone. In the latest stage intrusion of the Syringa Dikes.

2. 52 to 50 Ma. Motion on the Kettle River fault and intrusion of the most easterly of the "Coryell" syenites plutons (ex. Ymir).
3. 50 to 49 Ma. Intrusion of the Coryell Batholith. Probably simultaneously with the Granby Pluton.
4. 48 Ma to ? Motion on the west-dipping Granby River fault and some other fault(s) located east of the Kettle River fault. Some detailed geological or reflection seismic work in the area can establish the presence (or absence) of such west-dipping fault(s).

CHAPTER IV. GENERAL CONCLUSIONS

This thesis addresses two general tectonic problems in the Canadian Cordillera : post-Late Cretaceous latitudinal displacement of allochtonous terranes and Eocene extension in the Omineca Belt.

In the case of the terrane displacement (Chapter II), the new data from the Carmacks group are consistent with northward displacement of Baja British Columbia after latest Cretaceous time, in agreement with estimates of dextral motion on the Tintina-Northern Rocky Mountain Trench fault (Gabrielse, 1985) and plate tectonic models (Engebretson, 1985; Umhoefer, 1987). An important uncertainty that remains to be resolved is the estimate of the earlier part of the northward motion of Baja British Columbia. To do so, paleomagnetic work on *volcanic* Middle Cretaceous units from the western Cordillera has to be done, to check if the shallow paleolatitudes observed from the Cretaceous intrusions (Irving *et al.*, 1985) are not partly caused by geological tilt. Paleomagnetic work on other Late Cretaceous units would also be useful to verify the Carmacks' data and to clarify the situation about the rotation, since the rotation estimate in this study has a very large error. Paleomagnetic data from the Carmacks group brings us one step closer to a realistic

palinspastic reconstruction on the western Cordillera.

Work on the Eocene extensional process in the southern Omineca Belt is still at its first stages. Some geochronological work has been done (Carr *et al.*, 1987; Parrish *et al.*, 1988) and Bardoux and Irving (in preparation) and this thesis (Chapter III) presented paleomagnetic data indicating tilts. My interpretation of the eastward tilt of the Coryell Batholith is somewhat speculative : I had to infer the presence of a west-dipping fault east of the Coryell Batholith to explain the data. This is entirely possible, but such fault(s) have not been recognized yet. Maybe this data will encourage some geologist to look for them...

Nevertheless, the agreement of the data from the Granby Pluton and, to a lesser extent, the Syringa dikes with the extensional model of Parrish *et al.* (1988) shows that paleomagnetism is a potentially powerful tool for the determination of geological tilt in plutonic and metamorphic rocks of mid-crustal origin that otherwise have no evidence of paleohorizontal.

BIBLIOGRAPHY

AITKEN, J.D. 1959. Atlin map-area, British Columbia. Geological Survey of Canada, Memoir 307.

BARDOUX, M. and IRVING, E. Paleomagnetism of Tertiary rocks of the upper plate of the Okanagan crustal shear, Kelowna, British Columbia. In preparation.

BECK, M.E., Jr. 1976. Discordant paleomagnetic pole positions as evidence of regional shear in the Western Cordillera of North America. American Journal of Science, 276: 694-712.

BECK, M.E., Jr., BURMESTER, R.F., and SCHOONOVER, R. 1981a. Paleomagnetism and tectonics of the Cretaceous Mount Stuart batholith of Washington: translation or tilt? Earth and Planetary Science Letters, 56: 336-342.

BECK, M.E., Jr., BURMESTER, R.F., ENGEBRETSON, D.C., and SCHOONOVER, R. 1981b. Northward translation of Mesozoic batholiths, western North America: Paleomagnetic evidence and tectonic significance. Geofisica Internacional, 20: 143-162.

BOSTOCK, H.S. 1936. Carmacks District, Yukon. Geological Survey of Canada, Memoir 189.

BROWN, R.L., and JOURNEAY, J.M. 1987. Tectonic denudation of the Shuswap metamorphic terrane of southeastern British Columbia. Geology, 15: 142-146.

BULTMAN, T.R. 1979. Geology and tectonic history of the Whitehorse Trough west of Atlin, British Columbia. Ph.D. thesis, Yale University, New Haven, CT.

CAMPBELL, R.B. 1967. Reconnaissance geology of the Glenlyon map-area, Yukon Territory, Geological Survey of Canada, Memoir 352.

CARR, S.D., PARRISH, R.R., and BROWN, R.L. 1987. Eocene structural development of the Valhalla Complex, southeastern British Columbia. Tectonics, 6: 175-196.

CHURCHILL, S.J. 1980. Geochronometry and chemistry of the Cretaceous Carmacks group, Yukon. B.Sc. thesis, University of British Columbia, Vancouver, BC.

CREER, K.M. 1959. A.C. Demagnetization of unstable Triassic Keuper Marls from southwest England. Geophysical Journal of the Royal astronomical Society, 2: 261-275.

COX, A. 1957. Remanent magnetization of lower to middle Eocene basalts flows from Oregon. Nature, 179: 685-686.

COX, A. 1969. Confidence limits for the precision parameter *k*. Geophysical Journal of the Royal astronomical Society, 18: 545-549.

COX, A. 1980. Rotation of microplates in western North America. *in* The Continental Crust and its mineral deposits, Geological Association of Canada, Special Paper 20.

COX, A., and HART, R.B. 1986. Plate tectonics: how it works . Palo Alto: Blackwell Scientific Publications, 392 p.

DARLYMPLE, G.B., and LANPHERE, M.A. 1969. Potassium-Argon dating: Principles, techniques, and applications to geochronology. San Francisco, W.H. Freeman and Co.

DEBICHE, M., COX, A., and GORDON, R.G. 1985. The motion of allotochtonous terranes across the North Pacific Basin. Geological Society of America, Special paper 207.

DEMAREST, H.H. 1983. Error analysis for the determination of tectonic rotation from paleomagnetic data. Journal of Geophysical Research, 88: 4321-4328.

DIEHL, J.F., BECK, M.E., Jr., BESKE-DIEHL, S., JACOBSON, D., and HEARN, B.C., Jr. 1983. Paleomagnetism of the Late Cretaceous-early Tertiary north-central Montana Alkalic Province. Journal of Geophysical Research, 88:10 593-10 609.

ENGEBRETSON, D.C., COX, A., and GORDON, R.G. 1985. Relative motions between oceanic and continental plates in the Pacific Basin. Geological Society of America, Special paper 206.

FYLES, J.T. 1984. Geological setting of the Rossland mining camp. British Columbia Ministry of Energy, Mines and Petroleum Resources, Bulletin 74.

GABRIELSE, H. 1985. Major dextral transcurrent displacements along the Northern Rocky Mountain Trench and related lineaments in north-central British Columbia. Geological Society of America Bulletin, 96: 1-14.

GABRIELSE, H., DODDS, C.J., MONGER, J.W.H., and YORATH, C.J. 1988. Regional transcurent faults in the Canadian Cordillera. American Geophysical Union, Special Paper. In press.

GORDON, R.G., COX, A., and O'HARE, S. 1984. Paleomagnetic Euler poles and the apparent polar wander and absolute motion of North America since the Carboniferous. Tectonics, 3: 499-537.

GROND, H.C. 1980. New K-Ar dates and geochemistry for Mount Nansen Volcanics, Yukon. B.Sc. thesis, University of British Columbia, Vancouver, BC.

GROND, H.C., CHURCHILL, S.J., ARMSTRONG, R.L., HARAKAL, J.E., and NIXON, G.T. 1984. Late Cretaceous age of the Hutshi, Mount Nansen, and Carmacks groups, southwestern Yukon Terrotory and northwestern British Columbia. Canadian Journal of Earth Sciences, 21: 554-558.

HANNA, W.F. 1967. Paleomagnetism of Upper Cretaceous volcanic rocks of southwestern Montana. Journal of Geophysical Research, 72: 595-610.

HARLAND, W.B., COX, A.V., LLEWELLYN, P.G., PICKTON, C.A.G., SMITH, A.G., and WALTERS, R. 1982. A geologic time-scale. Camridge, Cambridge University Press.

HILLHOUSE, J.W., and GROMME, C.S. 1982. Limits to northward drift of the Paleocene Cantwell Formation, Central Alaska. Geology, 10: 552-536.

IRVING, E. 1964. Paleomagnetism and its application to geological and geophysical problems. New York: J. Wiley and sons, 399 p.

IRVING, E. 1979. Paleopoles and paleolatitudes of North America and speculation about displaced terrains. Canadian Journal of Earth Sciences, 16: 69-694.

IRVING, E. 1985. Whence British Columbia? Nature, 314: 673-674.

IRVING, E., and IRVING, G.A. 1982. Apparent polar wander paths Carboniferous through enozoic and the Assembly of Gondwana. Geophysical Surveys, 5: 141-188.

IRVING, E. and WYNNE, P.J. 1988. Paleomagnetic evidence for motions of parts of the Canadian Cordillera. Tectonophysics (in press).

IRVING, E., WYNNE, P.J., and WOODSWORTH, G.J. 1985. Paleomagnetic evidence for displacement of the Coast Plutonic Complex, British Columbia. Canadian Journal of Earth Sciences, 22: 584-598.

LITTLE, H.W. 1957. Kettle River, east half, British Columbia. Geological Survey of Canada: map 6-1957.

LITTLE, H.W. 1960. Nelson map-area, west half, British Columbia. Geological Survey of Canada : memoir 308.

LITTLE, H.W. 1982. Geology of the Rossland-Trail map-area, British Columbia. Geological Survey of Canada, Paper 79-26.

LOVLIE, R., and OPDYKE, N.N. 1974. Rock magnetism and paleomagnetism of some intrusions from Virginia. Journal of Geophysical Research, 79: 343-349.

LOWEY, G.W., SINCLAIR, W.D., and HILLS, L.V. 1986. Additionnal K-Ar isotopic dates for the Carmacks group (Upper Cretaceous), west central Yukon. Canadian Journal of Earth Sciences, 23: 1857-1859.

LOWRIE, W., and FULLER, M. 1971. On the alternating field demagnetization characteristics of multidomain thermoremanent magnetization in magnetite. Journal of Geophysical Research, 76: 6339-6349.

McFADDEN, P.L., and JONES, D.L. 1981. The fold test in paleomagnetism. Geophysical Journal of the Royal astronomical Society, 67: 53-58.

McFADDEN, P.L., and McELHINNY, M.W. 1984. A physical model for paleosecular variation. Geophysical Journal of the Royal astronomical Society, 78: 809-830.

MONGER, J.W.H., and BERG, H.C. 1987. Lithotectonic terrane map of western Canada and southeastern Alaska. U.S. Geological Survey, Misc. Field Studies Map 1874-B.

MONGER, J.W.H., PRICE, R.A., and TEMPLEMAN-KLUIT, D.J. 1982. Tectonic accretion and the origin of the two major metamorphic and plutonic welts in the Canadian Cordillera. Geology, 10: 70-75.

PARRISH, R.R. 1984. Slocan Lake fault: a low angle fault zone bounding the Valhalla Complex, Nelson map area, southern British Columbia. Geological Survey of Canada, Paper 84-1A: 323-330.

PARRISH, R.R., CARR, S.D., and PARKINSON, D.L. 1988. Eocene extensional tectonics and geochronology of the Southern Omineca Belt, British Columbia and Washington. Tectonics, in press.

RODDICK, J.A. 1967. Tintina Trench. Journal of Geology, 75: 23-33.

SHIVE, P.N., and PRUSS, E.F. 1977. A paleomagnetic study of basalt flows from the Absaroka Mountains, Wyoming. Journal of Geophysical Research, 82: 3039-3048.

STEIGER, R.H., and JÄGER, E. 1977. Subcommission on geochronology: Conventions on the use of decay constants in geo- and cosmochronology. Earth and Planetary Science Letters, 36: 359-362.

TEMPLEMAN-KLUIT, D.J. 1974. Geology of the Carmacks map-area, Yukon Territory. Geological Survey of Canada, Open File 200.

TEMPLEMAN-KLUIT, D.J. 1976. The Yukon Crystalline Terrane: enigma in the Canadian Cordillera. Geological Society of America Bulletin, 87: 1343-1357.

TEMPLEMAN-KLUIT, D.J. 1978. Laberge map-area, Yukon Territory. Geological Survey of Canada, Open File 578.

TEMPLEMAN-KLUIT, D.J. 1980. Highlights of field work in Laberge and Carmacks map-areas, Yukon Territory. Geological Survey of Canada, Paper 80-1A: 357-362.

TEMPLEMAN-KLUIT, D.J. 1984. Geology, Laberge (105E) qnd Carmacks (115I), Yukon Territory. Geological Survey of Canada, Open File 1101.

THELLIER, E. 1937. Sur la disparition de l'aimantation permanente des terres cuites par réchauffement en champ magnétique nul. Compte rendus de l'Académie des Sciences de Paris, 205: 334-336.

TIPPER, H.W., WOODSWORTH, G.J., and GABRIELSE, H. 1981. Tectonic assemblage map of the Canadian Cordillera and adjacent parts of the United States of America. Geological Survey of Canada, Map 1505A.

UMHOEFER, P.J. 1987. Northward translation of "Baja British Columbia" along the Late Cretaceous to Paleocene margin of western North America. Tectonics, 6: 377-394.

VUGTEVEEN, R.W., BARNES, A.E., and BUTLER, R.F. 1981. Paleomagnetism of the Roskruge and Gringo Gulch Volcanics, southeast Arizona. Journal of Geophysical Research, 86: 4021-4028.

WATSON, G.S. 1956. Analysis of dispersion on a sphere. Monthly Notices of the Royal astronomical Society, Geophysical Supplement, 7: 153-159.

WHEELER, J.O. 1961. Whitehorse map-area, Yukon Territory. Geological Survey of Canada, Memoir 312.

WHEELER, J.O., and McFEELY, P. 1987. Tectonic assemblage map of the Canadian Cordillera and adjacent parts of the United States of America. Geological Survey of Canada, Open File 1565.

ZIJDERVELD, J.D.A. 1967. A.C. demagnetization of rocks: analysis of results. In Methods in Paleomagnetism (Collinson, D.W. and Creer, K.M., eds). Amsterdam: Elsevier Publishing Company, 254-286.

VITA

Surname : Marquis Given Name: Guy

Place of birth: Gagnon Date of birth: April 2, 1965

Educational Institutions Attended, with dates of Entering and Leaving:

UNIVERSITE DU QUEBEC A CHICOUTIMI 1983 to 1986

UNIVERSITY OF VICTORIA, B.C. 1986 to 1988

Degrees, Diplomas, Etc., Awarded and names of Institutions:

B.Sc. 1986 Université du Québec à Chicoutimi

Honors and Awards:

Fonds F.C.A.R. Scholarship, 1986/87 and 1987/88

University of Victoria Supplement, 1987/88

Publications:

MARQUIS, G. and GLOBERMAN, B.R. Nothward displacement of the Whitehorse Trough, paleomagnetic evidence fron the Upper Cretaceous Carmacks Group. Accepted by the Canadian Journal of Earth Sciences.

PARTIAL COPYRIGHT LICENSE

I hereby grant the right to lend my thesis (the title of which is shown below) to users of the University of Victoria Library, and to make single copies only for such users or in response to a request from the Library of any other university, or similar institution, on its behalf or for one of its users. I further agree that permission for extensive copying of this thesis for scholarly purposes may be granted by me or a member of the University designated by me. It is understood that copying or publication of this thesis for financial gain shall not be allowed without my written permission.

Title of Thesis

Aberrant paleomagnetic directions in the Canadian Cordillera

Author [redacted]

GUY MARQUIS

March 17, 1988